

University of Hohenheim

Faculty of Agricultural Sciences

Institute for Plant Production and Agroecology in the Tropics and Subtropics

Crop Waterstress Management in the Tropics and Subtropics



**Species-Specific Estimation of Above-Ground Carbon Density by
Optical *In Situ* Measurements of Light Interception in Semi-Arid
Grasslands**

Christina Seckinger

M.Sc. Thesis

This work was financially supported by the GIZ



Main-supervisor: Prof. Dr. Folkard Asch

Co-supervisor: Prof. Dr. Roland Gerhard

Hohenheim, August 2014

Zusammenfassung

Die Menschheit als Teil des Erdsystems hat im Zuge der Industrialisierung immer weiter zunehmend an Einflussgröße gewonnen. Die Verbrennung fossiler Energieträger sowie die Änderung und Intensivierung der Landbewirtschaftung, welche dem Bevölkerungswachstums geschuldet ist, führen zu einer fortschreitenden Anreicherung von klimawirksamen Emissionen in der Atmosphäre. Dieser Wandel kann aufgrund von Interaktionsmechanismen nur schwer abgeschätzt und bei Überschreitung von Schwellenwerten auch nur bedingt wieder rückgängig gemacht werden. Eine Stellschraube stellt die Anreicherung von Kohlenstoff in terrestrische Ökosysteme dar, welche mithilfe von unterschiedlichen Managementmethoden weiter gesteigert werden kann. Seit ein paar Jahrhunderten kommt es in vielen Teilen halbtrockener Savannen zu einer Änderung der Artenzusammensetzung hin zu mehr verholzenden Arten, wodurch zusätzlicher Kohlenstoff durch eine Verschiebung aus der Atmosphäre in die Biosphäre klimaneutral gebunden wird. Der Verlust an wertvoller Weidefläche für die dort ansässige Landbevölkerung steht diesem relativ neuen landschaftlichen Erscheinungsbild gegenüber. Für die Einführung von Transferzahlungen in Form von Zahlungen für Umweltdienstleistungen (PES) müssen Methoden gefunden werden, die effizient und großräumig, die potentiellen Flächen auf die vorhandene Biomasse, abschätzen können. In dieser Arbeit wurden die am häufigsten dort vorkommenden Arten mithilfe destruktiver und nicht-destruktiver Methoden auf ihre Biomasse näher untersucht. Der optische Sensor des Messgerätes LAI-2000 PCA diente zur Bestimmung der Projektionsfläche der Pflanzenbestandteile. Mit dieser gewonnenen Messgröße wurde unter Berücksichtigung der destruktiv gemessenen Biomasse die artspezifische Biomasse versucht abzuschätzen daneben wurde auch die räumliche Verteilung der Kohlenstoffdichte in unterschiedlichen Vegetationstypen ermittelt.

Acknowledgment



Thanks to all the people who have walked this seemingly endless path with me.

Table of Contents

Zusammenfassung	II
Acknowledgment.....	III
Table of Contents	IV
List of Figures.....	VII
List of Tables	VIII
List of Abbreviations	IX
1. Introduction	1
1.1. Motivation	1
1.2. Background	2
1.3. Main Objectives	3
2. Literature Review	4
2.1. Measurement Methods to Determine Above-ground Biomass	4
2.2. Climate Change and the Global Carbon Cycle	6
2.3. Terrestrial Ecosystems	8
2.3.1. Tropical grasslands	9
2.3.2. Encroachment	10
3. Materials	12
3.1. Study Area.....	12
3.2. Experimental Set-up.....	14
4. Methods	15
4.1. The Measurements of Different Plant Parameters	15
4.2. Destructive Volumetric Biomass Determination	16
4.3. Determination of Leaf Area, by Image Analysis	17
4.4. Determination of the Clumping Index	18
4.5. Non-destructive Methods	19
4.5.1. Instrument description	19
4.5.2. Indirect measurements of the biomass by LAI-2000 PCA.....	20

4.5.3.	Software FV2000 for further processing of the acquired field data	22
4.5.4.	Projection to the bottom	23
4.5.5.	Determination of the AGB by optical based method	25
4.6.	Statistical Analyses	27
5.	Results	29
5.1.	Destructive Methods	29
5.1.1.	Canopy density of the species	29
5.1.2.	Specific leaf area values of the species	30
5.1.3.	Leaf area density.....	31
5.2.	Non-destructive Methods´	33
5.2.1.	Relationship of species-specific plant area density as measured by LAI-2000 PCA	33
5.2.2.	The compare of canopy density to plant area density for each species.....	34
5.2.3.	Destructive and non-destructive measurements of canopy density and area	35
5.2.4.	Influence of wood density and leafs to the optical measured total plant area	36
5.2.5.	Summary (1).....	37
5.2.6.	Pooled data	38
5.3.	Species-specific Above-ground Biomass Estimation	40
5.3.1.	Methods comparision	40
5.3.2.	The comparision of the different species.....	42
5.3.3.	Influence of increasing leaf area on the above-ground biomass	44
5.3.4.	Summary (2).....	45
5.4.	Consideration of the Canopy Structure	46
5.4.1.	Ratio of canopy density to plant area density.....	46
5.4.1.	Species-specific clumping index	47
5.4.2.	Estimation of spatial carbon density distribution on plot level	49
5.4.3.	Summary (3).....	51
6.	Discussion.....	52

7. Conclusion.....	55
References	X
List of Appendix Contents.....	XXIII

List of Figures

Fig. 1: Simple and basic design of the most important carbon pools and fluxes in the global carbon cycle.....	6
Fig. 2: Climate diagram of the Borana zone.....	12
Fig. 3: Spatial distribution of the different vegetation type plots in the research area.	12
Fig. 4: Destructive harvesting of the canopy density	16
Fig. 5: Image processing.....	17
Fig. 6: Sensor head with the 5 viewing angles of the LAI-2000 Plant canopy analyzer.....	19
Fig. 7: Canopy structure considered from the bottom to the top.....	20
Fig. 8: Illustrates the DISTS vector in the side view with the 5 viewing angles.....	24
Fig. 9: Chart of travel paths for the measurements with the	25
Fig. 10: Canopy density of the different species	29
Fig. 11: Change in leaf area density.	31
Fig. 12: Species-specific plant area density.....	33
Fig. 13: Species-specific plant area density.....	34
Fig. 14: Destructive and non-destructive measurements over the trail time.	35
Fig. 15: Regression line of canopy density	38
Fig. 16: Regression line of squared canopy density	39
Fig. 17: Species specific regression lines of AGB	42
Fig. 18: Plot of studentized residual obtained from regression analyses versus increasing leaf area.....	44
Fig. 19: The ratio of canopy density to plant area density	46
Fig. 20: Carbon content for each grid point.....	50

List of Tables

Table 1: Summary of the measured species and the bush-tree-savanna plots around on which the measurements were performed.....	14
Table 2: Field set-up and position modifications of the four methods.....	21
Table 3: Summary of the modifications in the field and further handling of the software application FV2000.	23
Table 4: Specific leaf area values of the different species	30
Table 5: Clumping effect of each species.....	48

List of Abbreviations

AGB	above-ground biomass; destructive
C	carbon
CD	canopy density; destructive
cm	centimeter
g	gram
Fig.	figure
LAI	leaf area index; destructive
LD	leaf area density; destructive
DLLAI	drip line leaf area index
DLPAI	drip line plant area index; non-destructive
Ln	natural logarithm
m	meter
mm	millimeter
PAI	plant area index;
PAI_e	effective plant area index; non-destructive
PD	plant area density; non-destructive
Pg	petagram
ppm	parts per million
r	radius
rep	repetition
SAI	stem area index; destructive
SLA	specific leaf area, destructive
SD	standard derivation
y	year

1. Introduction

1.1. Motivation

The Earth System can be differentiated into different parts, called spheres. These spheres overlap each other and hence do not occur in isolation [Bockheim et al., 2010]. The abiotic parts of these spheres are separated into the hydrosphere, the lithosphere, the pedosphere, and the atmosphere. The living world is defined as the biosphere, a sphere which can be present in any of the other open sphere systems [Claussen, 2002]. Regarding mass exchange, the Earth is an almost closed system but this is not the case regarding energy exchange. The electromagnetic radiation of the sun is the primary energy source for the Earth [Jacobson et al., 2000; Steffen et al., 2004]. The dynamic of the Earth System results in a permanent flow and transformation of atoms and chemical compounds within one of the mentioned spheres or between these various spheres. These fluxes can be described by individual biogeochemical cycles (e.g. carbon cycle; nitrogen cycle) [Jacobson et al., 2000]. The biogeochemical cycles, as well as the behavior of energy in the system, are complex, dynamic and interspersed with chemical, physical and biological processes. [Steffen et al., 2004]. Long-time records of the atmosphere CO₂ concentration clearly indicate an anthropogenic impact on the Earth System [Vitousek et al., 1997]. This results in an increasing demand in practices which mitigate the effects of progressive climate change like carbon sequestration or the reduction of anthropogenic emissions [Ingram and Fernades, 2001].

1.2. Background

The study [under discussion in this paper] was conducted in the Borana zone, Southern Ethiopia, within the framework of the project “Livelihood diversifying potential of livestock based carbon sequestration options in pastoral and agro-pastoral systems in Africa”. It was funded by the BMZ (Federal Ministry of Research and Education), coordinated by ILRI (International Livestock Research Institute) and implemented in cooperation with the DITSL in Kassel (German Institute for Agriculture in the Tropics and Subtropics), the University of Hawassa, Ethiopia, and the University of Hohenheim, Germany. The goal of this project was to assess the potential of pastoral and agro-pastoral systems to sequester carbon. Furthermore, its aim was to explore the impact of decision-making in regard to land-use and livestock management techniques with a potential reduction of carbon emissions and a mitigation of the climate change.

The people of the pastoral and agro-pastoral communities in the semi-arid savannas of the Borana zone in Southern Ethiopia are mainly depending on livestock for their livelihood. These traditional livestock-based systems are under extreme pressure, amongst others, through structural changes, triggered by the population growth, resource scarcity and weather extremes. There is a need to diversify the livelihood of the pastoralist so as to overcome the vulnerability of these systems and to counteract poverty. Payments for Environmental Services (PES), based on the reduction of carbon emissions and the carbon sequestration potential linked to rangeland management practices, present one option for diversification in order to overcome the vulnerability of these systems. On the one hand, the introduction of PES into these systems is an option to provide additional income sources for the pastoralist, and, on the other hand, it contributes to the reduction of greenhouse gas emissions. Carbon is stored in dead and living biomass in the soil, in living biomass and in litter above-ground [Hairiah et al., 2001]. The focus of this study lies on the estimation of living above-ground biomass by the implementation of destructive and non-destructive methods.

1.3. Main Objectives

In order to introduce clean development mechanisms, like PES in the Borana zone, the region of the study under discussion, an analysis on the current carbon quantity and its allocation is required. This study focuses on the estimation of seasonal above-ground biomass allocation in different savanna vegetation types and dominant woody species by using destructive as well as non-destructive methods.

Specific objectives were:

1. An analysis of the seasonal above-ground biomass dynamics (end of dry season until end of rainy season) of different savanna vegetation types: grass-savanna, bush-savanna, tree-savanna and bush-tree-savanna and the species-specific consideration of above-ground biomass of dominant woody species: *A. bussei*, *A. nilotica*, *A. nubica*, *A. tortilis*, and *Achyr. aspera*.
2. The evaluation of a non-destructive method to assess above-ground biomass through the LAI-2000 PCA.
3. The identification and analysis of influencing factors adjunct to the measurement with the LAI-2000 PCA.

2. Literature Review

2.1. Measurement Methods to Determine Above-ground Biomass

“Biomass is defined as the total amount of above ground living organic matter for example in trees expressed as oven-dry tons per unit area.” (FAO)¹

There is a high spatial and temporal variability of biomass [Lu, 2006; Houghton et al., 2009]. Above-ground biomass (AGB) could be further subdivided into woody biomass and foliage biomass [Franklin and Hiernaux, 1991]. Most methods for biomass estimation are methods to measure the above-ground biomass. The determination of the AGB mainly takes place either by remote sensing methods or by using in situ field measurements methods which can further be separated into direct and indirect ones [Lu, 2006]. The direct estimation of AGB is the destructive harvesting and weighting of plant material. The destructive harvest method involves a considerable workload to obtain a set of plant variables which are correlated to AGB by simple regression equations [Northup et al., 2005]. Stem diameter of trees are often related to woody biomass and canopy volume is related to foliage biomass in semi-arid woodlands [Poupon, 1977; Cissé, 1980]. For bushy shrub species, canopy volume is also a good predictor for AGB [Hasen-Yusuf et al., 2013], consequently, the indirect estimation of AGB in situ by allometric equation is invariably based on previously destructive methods. In general, the AGB of trees and shrubs of the site under study is extrapolated [Jonckheere et al., 2003]. Remote sensing can be separated into passive and active methods. The estimation of AGB itself, by remote sensing methods, takes place direct or indirect. As related to the direct method, its data set of AGB is often linked to regression analysis, whereas for the indirect method, data are used to obtain other canopy information. Information about the structure of canopy is more exactly detectable and can also be correlated to AGB (e.g. allometric equations) [Lu, 2006]. The multi-frequency polarimetric synthetic aperture radar (SAR), for example, is an active remote sensing method. The data set was used to determine the biomass in Australian savannas. The study observed that the regression analysis showed a strong relationship between backscatter intensity and biomass, which was estimated by allometric equations [Collins et al., 2009]. Another example is the MODIS satellite observation data set

¹<http://www.fao.org/docrep/009/j9345e/j9345e12.htm>

in the study of Baccini et al. [2008] which was used to estimate AGB in Africa to create a biomass map.

2.2. Climate Change and the Global Carbon Cycle

In the tropics, the response of ecosystems to climate change shows that tropical ecosystems change even before a change in climate, e. g. in temperature, is recorded [Marchant et al., 2006]. The global carbon cycle is the biogeochemical cycle with the highest turnovers rates regarding mass and energy, and it is closely linked to the climate system [Ciais et al., IPCC 2013]. The temporal dynamic reservoirs - with large carbon fluxes and turnover time scales of years to decades to centuries – are: the atmosphere (turn over time scales of years); the oceans, in particular with regard to the upper layer (e.g. surface ocean sediments); the freshwater reservoirs; the terrestrial ecosystems, which consist of soils and vegetation (turn over times scales of decades to centuries e.g. agriculture development); and fossil fuel reserves [Ciais et al., IPCC 2013; Houghton et al., 2009].

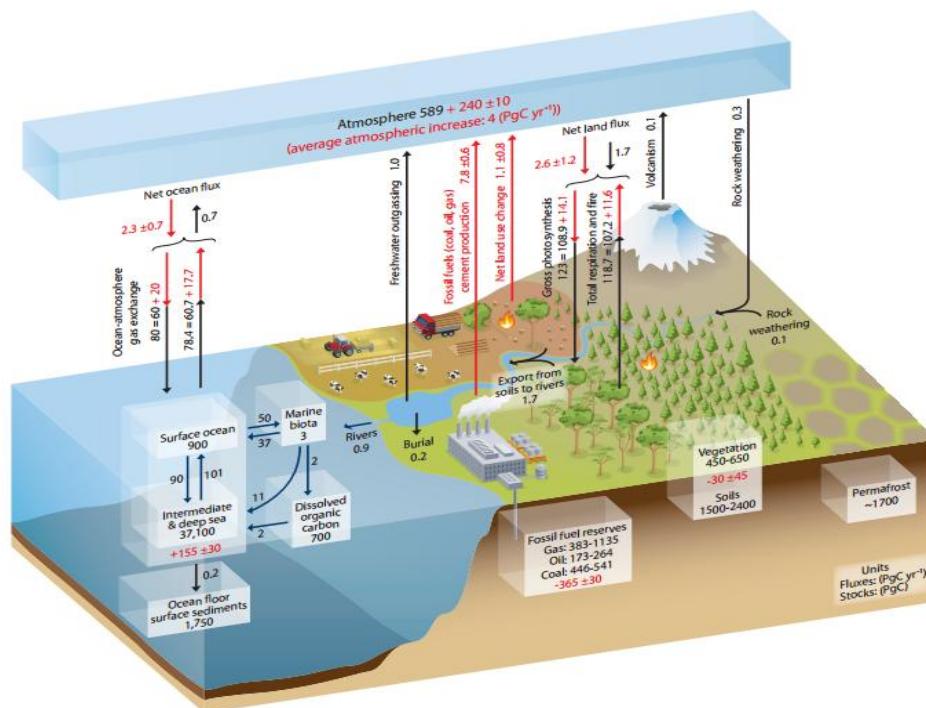


Fig. 1. Simple and basic design of the most important carbon pools [PgC] and fluxes [PgC yr⁻¹] in the global carbon cycle. Black colored for pool sizes and fluxes in the Pre-Industrial Era and red colored for cumulative carbon [PgC] in the time frame of 1750 to 2011 plus the time-averaged fluxes [PgC yr⁻¹] over the years 2000 to 2009. [Ciais et al., IPCC 2013: The Physical Science Basis, Intergovernmental Panel on Climate Change]. Estimated amounts of the carbon pools and related fluxes for the pre-industrial time are shown in numbers and arrows colored black; however the cumulative amount of carbon [PgC] in the time frame of 1750 to 2011 and carbon fluxes [PgC yr⁻¹] which are time-averaged values over the observation years of 2000 to 2009 are colored red. Negative and positive values indicate a source or a sink of carbon [Ciais et al., IPCC 2013].

In the year 2004, 80% of world's population were living in the developing and in the least-developed countries. These countries are mostly responsible for the increase of the anthropogenic CO₂ emissions. However, in a quantitative term, less than half of the CO₂ emissions originate from these economies. A look at the cumulative emissions (1750 to 2004) shows that these countries only contribute 23 % to the global cumulative emissions [Raupach et al., 2007]. Carbon fluxes from the Lithosphere (e.g. rocks) caused by erosion and weathering, as well as the buffering effect of CO₂ caused by sedimentation of carbon particles on the ocean surface floor [Sundquist, 1990], are domains of the earth system with large turnover times and smaller fluxes. For millennia, approximately 0.2 PgC accumulates in carbonate sediments on the ocean floor every year [Sabine et al., IPCC 2013; Denman et al., IPCC 2007]. Fossil carbon was a slow reservoir of carbon in the pre-industrial era but has been transferred to a fast domain of carbon, with large fluxes to the other reservoirs, until now [Ciais et al., 2013, IPCC 2013]. This is due to the fact that fossil energy covered 78% of the global energy demand in 2005 [GEA, 2012]. The most important reservoirs (PgC) and fluxes (PgC y⁻¹) are illustrated in Fig. 1. Two kinds of sources contributed to a cumulative amount of 550 PgC of anthropogenic carbon emissions from 1750 to 2011. The major part results from the consumption of fossil fuel for energy demand and from the industrial cement production. The smaller part with 180 PgC is a consequence of land use change (LUC) [Ciais et al., 2013, IPCC 2013]. Only in Africa, emissions from fossil fuel are lower than through LUC [Valentini et al., 2013]. The conversion factor for 1 ppm CO₂ (Volume) is 2.12 PgC [Prather et al., 2012]. 240 PgC remain in the atmosphere [Ciais et al., IPCC 2013]. In April, 2014 the monthly average value of atmospheric CO₂ exceed 400 ppm in Mauna Loa². The global CO₂ concentration has been rising continuously. The growth rate of global CO₂ emissions has more than tripled from approximately 1-1.1 % (1990-1990) to 3.2-3.3% (2000-2004/2005), which represents an increase in >2 ppm y⁻¹ in atmospheric CO₂ concentration and thus also exceeded the annual emission growth rates which were based on the worst case scenario [Raupach et al., 2007], called A1F1 [IPCC, 2000]. The ocean is the greatest sink for CO₂ emissions and accumulated 155 PgC of the emissions caused by human activity between 1750-2011 [Ciais et al., IPCC 2013]. The terrestrial ecosystems could be a sink or a source for carbon. Ecosystems, which are not affected by land use change accumulate 160 PgC, which is defined a residual land sink [Ciais et al. 2013, IPCC 2013].

²<http://www.esrl.noaa.gov/gmd/ccgg/trends/index.html#mlo>

2.3. Terrestrial Ecosystems

The terrestrial ecosystems are complex systems. Plant photosynthesis as well as the respiration of autotrophic and heterotrophic organisms and carbon decomposition in the soil organic matter are processes in the global carbon cycle. These processes result in annual and inter-annual variability of the atmospheric CO₂ concentration [Cao and Woodward, 1998]. 25% of the inter-annual variability of the global carbon cycle is caused by the African continent [Valentini et al., 2013]. Biomass divided into above and below, litter, dead wood and soil organic matter are the carbon pools in terrestrial ecosystems [IPCC, 2006]. The total amount of above and below ground living biomass is between 773 and 1300 PgC, including the highest uncertainties in quantities which are caused by the estimation of forest biomass [Houghton et al., 2009]. The land-atmosphere flux (often abbreviated with land-flux) is the exchange of carbon between atmosphere and biosphere. It describes the balance of carbon release to the atmosphere and its uptake by the ecosystems [Schaphoff et al., 2006]. Consequently, the magnitude of the net-flux may be positive or negative. Positive net-land flux results in an increase of carbon in the atmosphere, negative net-land flux in a remove of carbon from the atmosphere. Since 1980, total net-land flux outweighs the net-land-use flux; in addition, the land-to-atmosphere flux shows a continuous rise and increased carbon storage in terrestrial ecosystems [Ciais et al., 2013, IPCC 2013], but rapid alteration has been taking place in environmental conditions, such as a larger N deposition, enrichment in the atmospheric CO₂ and increasing temperature. As a result, the carbon pool and net land flux of terrestrial ecosystems will be changing due to positive and negative feedback effects. For example, increased N deposition and atmospheric CO₂ concentration expand the terrestrial carbon pool [Bala et al., 2013]. An increase in temperature leads to increased respiration rates [Heimann et al., 2008] reducing the potential in carbon accumulation of the residual land sink. Additionally, the photosynthesis of plants is sensitive to the rising temperatures [Ciais et al., 2013, IPCC 2013] and the occurrence of respective climate feedback (e.g. the change in the distribution of precipitation and the total amount of evaporation) demonstrate the complexity of the interactions between the terrestrial carbon pool and the atmosphere and climate. This results in large uncertainties in the model [Ciais et al., 2013, IPCC 2013], including uncertainties in the magnitude of the net-land flux and in the role of the terrestrial ecosystems, being either a carbon sink or a source for carbon [Heimann et al., 2008] [Ciais et al., 2013, IPCC 2013]. The value of gross primary production is circa 120 PgC y⁻¹. Half of this is lost in the growth and maintenance processes of the plants. In 2000, the value of NPP through

photosynthesis was 59.22 PgC y^{-1} [Haberl et al., 2007]. A part of the above ground biomass falls to the ground. The leaf-litter and the soil organic matter are decomposed by microorganisms, thus reducing the remaining natural sequestered carbon. This is called a net ecosystem production (NEP). In the long-term view, disturbances, such as harvest and fire, may further reduce NEP. This production is defined as the net biome production (NBP) [Steffen et al., 1998]. Due to the effect that disturbances change carbon fluxes on different time scales, NEP and NBP are difficult to separate [Randerson et al., 2002]. Human activities reduce the potential NPP through the land use change (LUC). The harvested wood products and the induced fires further reduce the actual NPP; hence, in the year 2000, 15.6 PgC y^{-1} (23.8 %) of global NPP was lost by human appropriation with the highest loss in NPP attributed to the agricultural sector (cropping and grazing) [Haberl et al., 2007].

2.3.1. Tropical grasslands

The NPP of tropical savannas vary between 1 and $12 \text{ t C ha}^{-1} \text{ y}^{-1}$ [Grace et al, 2006]. In this ecosystem, the average density of living biomass is 57 Mg ha^{-1} (total amount 160 PgC). Tropical grasslands without trees reach average density values of 5 Mg ha^{-1} [Houghton et al., 2009]. The tropical grassland biome includes the tropical and subtropical grasslands, savannas and shrublands. Savannas cover an area of one-sixth of the terrestrial earth surface [Grace et al., 2006]. The African continent has the largest area of grasslands and savannas, exceeding the tropical rainforest area [Scurlock and Hall, 1998]. The reason for the worldwide large-spatial expansion of this ecosystem is that savannas occur in a wide range of climate conditions [Jeltsch and Grimm, 2000]. Competitive interactions and demographic bottleneck processes, related to the quantitative limitation of tree frequency, explain the coexistence of trees and grasses [Sankaran et al., 2005]. The buffering mechanisms in savannas lead to this long-term coexistence and prevent savannas to exceed specific threshold values, which would result in a transformation from savanna to grassland or from savanna to woodland. Buffering mechanisms to prevent the shift into woodland are, for example, fire or seed predators; whereas opposing mechanisms to prevent the shift into grassland are: the grazing effect or the dormancy mechanism of the seeds [Jeltsch and Grimm, 2000]. Main driving forces in semi-arid savanna ecosystems are land use change and climate change [Lohmann et al., 2012].

2.3.2. Encroachment

The study of the Borana lowland led to the conclusion that in this region threshold values were crossed and the local ecosystem was altered to a woody plant encroachment condition [Dalle and Isselstein, 2006]. This invasion of woody plants into the tropical grassland biome, especially under the arid and semi-arid conditions, has been observed on a global scale during the last centuries [Béltran-Przekurat et al., 2008]. Because of implementation of water points, the management of grazing in the Borana zone has been shifted in grazing intensity and spatial distribution [Angassa et al., 2006]. In 2012, Angassa et al. assumed that encroachment was enforced through fire suppressing. In the Borana zone a decrease in herbaceous biomass was detected and this reduction in biomass production was negatively correlated with increasing encroachment [Dalle and Isselstein, 2006]. The herbaceous species composition is significantly influenced by grazing managements [Angassa, 2012] and the inter-annual rainfall variability is one of the most important factors influencing the livestock population dynamics [Angassa and Oba, 2013]. Jackson et al., [2002] observed that the carbon increase is higher in drier locations. Encroachment enhances the above-ground carbon pool, but also alters the soil SOC of the below-ground carbon pool [Jobbágy and Jackson, 2000]. Nevertheless, for some locations the increase in C decreased linear with the increase of mean annual precipitation, and even resulted in positive net-land-atmosphere carbon fluxes. Blaum et al. [2006] observed that the perennial grass cover decreases, if the shrub cover increases. However, there was no negative correlation observed for annual grasses. Simulation of the encroachment effect of vegetation itself indicated changes of climate variables, such as the humidity and the temperature of the low atmosphere [Béltran-Przekurat et al., 2008]. Encroachment increases the number of shrub species in the landscape; hence the rooting depth increases as compared to systems with grass species dominated compositions [Jobbágy and Jackson, 2000]. Consequently, the effect of carbon transportation in the deeper soil layers (e.g. root biomass) could be indicated. The rainfall has also an effect on the vertical distribution of SOC: dry ecosystems have deeper SOC distributions [Jobbágy and Jackson, 2000]. Additional to the effect of rainfall, the topo-edaphic conditions and the management practices on the local level also influence the potential of carbon sequestration [Asner et al., 2003].

For East Africa, the predictions of climate models to precipitation are that rainfall in the short rainy season will very probably increase, but for the long rainy season no clear predictions could be found [Christensen et al., 2013]. The trend of change in incidence and duration of drought events is uncertain, and the conclusion, which was met in the AR4, that there is a

medium to high confidence in this trend, must be reduced to low confidence for this trend evaluation [Bindoff et al., 2013]. However, the negative impacts of environmental degradation (e.g. water shortage), eco-physiological change (e.g. encroachment effects) and climate change resulted in the need of additional income for the pastoralists [Kassahun et al., 2008].

3. Materials

3.1. Study Area

The study was conducted in the Borana zone, Regional State of Oromiya, in the south of

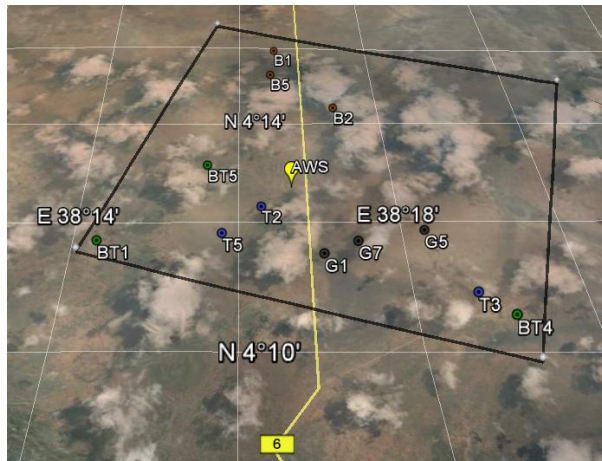


Fig. 3. Spatial distribution of the different vegetation type plots in the research area. G = grass, B = bush, BT = bush-tree and T = tree savanna.

Ethiopia. The Borana Rangeland covers an area of approximately 95 000 km² [McCarthy et al., 2001]. The Borana Plateau lies 1000-1600m above sea level. The landscape is mainly dominated by a semi-arid ecosystem with annual mean temperatures from 19 to 24°C and bimodal rainfall. Hence there are two rainy seasons which occur between March and May and between September and November. More precipitation is measured in the first rainy season than in the second [Coppock, 1993]. In both rainy seasons, the average rainfall of 353

mm to 873 mm (1982 -1996) is spatial and temporal highly variable [McCarthy et al., 2001].

The area under study had a size of 10 * 10 km, with the connecting road to Kenya running through it. A settlement with the name of Madhecho is located in the middle of this area. Since 07/16/2012, there is a weather station installed which records measured values for precipitation, radiation, temperature, relative humidity, wind speed and

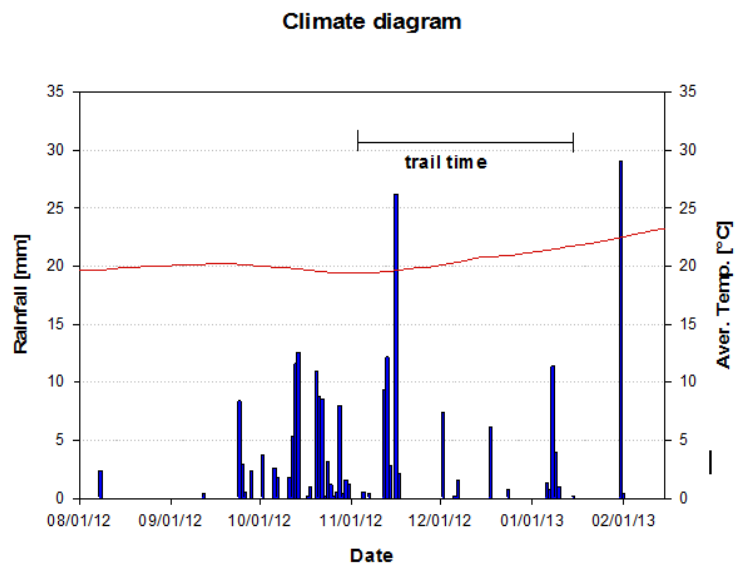


Fig. 2. Climate diagram of the Borana zone created by the data of the weather station in Madhecho.

wind direction, soil temperature in three different layers (10, 20 and 30 cm) and soil humidity in four different layers (10, 20, 30 and 40 cm). In the study area, four different vegetation types were distinguished and defined: grass-, bush-, bush-tree- and tree-savanna plots. Preliminary experiments, including LAI-2000 PCA measurements as well as selection and identification of the species and installation of marker points in the soil, took place in October 2012. The main experiment started on 11/04/2012 and ended on 01/15/2013.

3.2. Experimental Set-up

The selection of the species depended on the distribution of the species in the different vegetation types. In this study, the distribution of species within the bush-tree-savanna plots was considered in detail. *Acacia tortilis* (Forssk.) Hay. and *Acacia nilotica* (L.) Del. Var. *Nilotica* were common species on bush tree plots, which means they had an occurrence of 5-15%. The dominant species *Acacia bussei* Harms. ex. Sjöstedt reached a frequency of more than 15 % on the study area of bush-tree-savanna plots. Another species of bush, *Acacia nubica* Benth., was also common on BT plots (> 5-15 %) [Breuer, 2012]. Another shrub species was *Achyranthes aspera* L. Excluded from this study was *Acacia mellifera* Vahl Benth. also a common species on bush-tree-savanna plots [Breuer, 2012]. This species wasn't chosen because there were technical difficulties due to the spine structure. *Acacia tortilis* (Forssk.) Hay. and *Acacia nilotica* (L.) Del. Var. *Nilotica* and *Acacia bussei* Harms. ex. Sjöstedt. were measured destructive and non-destructive off-site the BT5-Plot. *Acacia nilotica* (L.) Del. Var. *Nilotica* was measured destructive and non-destructive off-site the BT4-Plot and *Achyranthes aspera* L. was measured destructive and non-destructive off-site the BT1-Plot, because appropriate samples for harvesting and non-destructive measurements of this species were not found in the vicinity of the other measured species. The following table (Table 1) summarizes this information. The soil type for each of the three bush-tree-savanna plots BT1, BT4, BT5 was the same, a Cambisol calcaric soil [Glatzle, 2012].

Table 1. Summary of the measured species and the bush-tree-savanna plots around on which the measurements were performed.

species list	bush-tree-savanna plots		
	BT1	BT4	BT5
<i>A. bussei</i>			x
<i>A. nilotica</i>		x	
<i>A. nubica</i>			x
<i>A.tortilis</i>			x
<i>Achyr. aspera</i>	x		

4. Methods

4.1. The Measurements of Different Plant Parameters

The trees and bushes were measured in four different vegetation types. The identification of plant species and the determination of different parameters, like perpendicular canopy radii, canopy height, total height and stem circumferences at ankle height, took place for each plot. The exact position of the species in the plot was conferred by the use of a compass, and the measuring of path lengths between species marker points installed at equal distances in the soil allowed an exact reconstruction of the plant positions at plot-level.

4.2. Destructive Volumetric Biomass Determination

A cube with the side length of 50 cm and open at all sides was custom-built by a metalworking shop. Accordingly, the volume was 0.125 m³. For the measurement, the tube was placed inside the canopy in such a way that it was completely filled with plant material. For every point of harvest given, three repetitions were chosen for every species. The vertical position of the cube was located between the center of the diameter and the outer edge, and the horizontal position was brought to the center of the total height for bush type species or to half of the crown height for tree type species. If the examined species had different habitus, these variations were tried to capture in their natural appearance. The selection of species



Fig. 4. Destructive harvesting of the canopy density [kg m⁻³].

repetitions has been done according to subjective and feasible criteria and does not claim to be complete in any way. Branches protruding out of the cube were removed by shears, and, after that, the content was cut out, while taking care that it was cut on the inside of the cube. The branches were separated between smaller than one cm and bigger than one cm. A sub-sample was removed from the entire sample. The leaves

of the sub-sample were placed on graph paper and photographed. Then these branches and the corresponding leaves were packed in separate envelopes and weighed with field scales with measurement scales from 0-60 g up to 600 g. The leaves of the remaining sample were also separated from the branches, packaged, and weighed. Fruits, flowers and recognizable growth of biomass was sorted out and recorded separately. The collected samples were first air dried and subsequently dried in a laboratory oven, (Binder GmbH, Tuttlingen, Germany) to a constant weight at 105 °C. A scale, (ADG 6000 L, Adam Equipment Co. Ltd, Milton Keynes, U.K.) with a resolution of 0.1 g and an accuracy of ±0.2, was used for weighing. Destructive harvesting was conducted every 2 weeks.

4.3. Determination of Leaf Area, by Image Analysis

The image processing and analysis program, ImageJ (National Institute of Health, USA), was used to determine the leaf area of the destructively harvested leaf samples. In the field, leaf samples were placed on scale paper and photographed with a digital camera. Image noise outliers were removed manually and the resulting image was split into three color channels (red, green, and blue). A reference length was set by using the grid lines of the scale paper. Subsequently, the grid lines of the scale paper were removed by eliminating the green and blue channels from the image. Each pixel was assigned a brightness value between 0 and 255, whereby an 8-bit grayscale image was created. Using the plug-in "Grayscale Morphology"³,

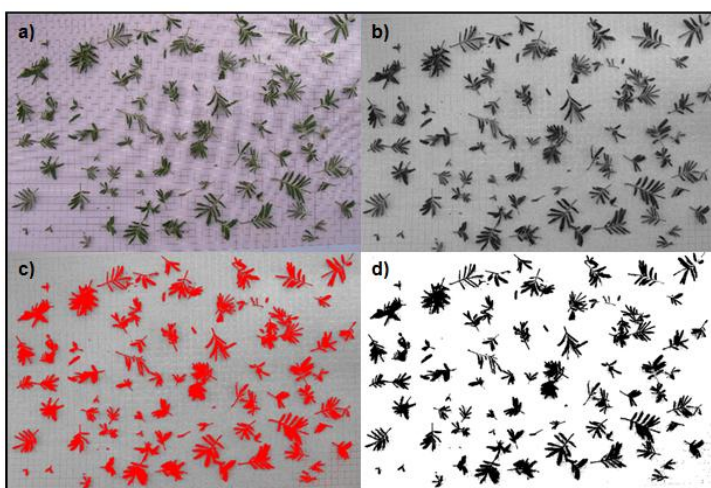


Fig. 5. Image processing a) initial image b) editing by splitting into color channels and grayscale morphology c) adjustment of the threshold value d) converting into binary.

which is based on different mathematical algorithms by using different structural elements and its size, the image quality increased and thus a more accurate measurement of the fine-textured leaf areas was achieved. After that, the image was converted into a binary image. The program ImageJ offered different ways of determining the threshold value for estimating the area covered

by the leaf. Eventually, the surface area of the leaves was calculated, and, together with the leaf biomass, also the specific leaf area (SLA) was determined.

³Prodanov, D., (2003). Grayscale Morphology

4.4. Determination of the Clumping Index

The clumping index was calculated with the help of the destructive measurements. The destructive woody biomass was separated into stems with smaller and larger than 1 cm diameter. The calculation of the cross section area was simplified by the hypothesis that the branches all shared the form of cylinders. The stem area index was corrected by wood density (kg m^{-3}). The Stem area index and the leaf area index resulted in the exact calculated plant area index.

The exact plant area index multiplied by the clumping index equals to plant area index obtained from the LAI-2000 PCA.

4.5. Non-destructive Methods

4.5.1. Instrument description

The LAI-2000 Plant Canopy Analyzer (LAI-2000 PCA), which is produced by Li-Cor Inc. (Lincoln, Nebraska, USA), is a device for the indirect optical based method to determine the leaf area index (LAI), the foliage density (PD), or the drip line leaf area index (DLLAI). However, all projected areas of opaque objects including stems, branches and fruit are detected by the sensor and hence the term plant area index (PAI) is more appropriate [Asner et al,

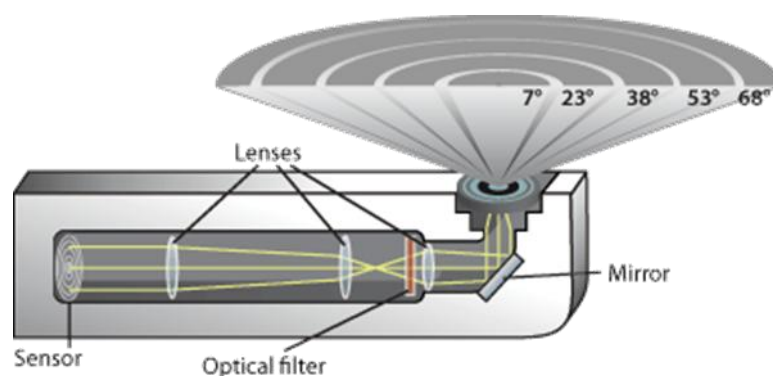


Fig. 6. Sensor head with the 5 viewing angles of the LAI-2000 Plant canopy analyzer; (Pictured is the sensor head of the LAI-2200).

2003; Welles and Norman, 1991]. The optical sensor of the LAI-2000 PCA device uses fish-eye lens. The almost hemispheric images viewed by the sensor are projected onto five detectors which are arranged in five concentric rings (Fig. 6). The device is able to operate with an azimuthally view of 360° for each ring (manual LAI-2000). In order to reduce the azimuthal view, different viewing caps are available which are useful for different environmental conditions (e.g. blocking direct sunlight or eliminating surrounding objects), or for special applications. Wavelengths above 490 nm are restricted with an optical filter within the sensor because higher wavelengths are based on volume scattering by foliage [Welles and Norman, 1991]. The LAI-2000 PCA measures the transmittance of light through the canopy at 5 separate zenith view angles (7° , 23° , 38° , 53° , 68°) and directly integrates the canopy's gap fraction for each ring by comparing in each ring above and below readings of the obtained measurements values [Wang et al., 1992]. The measurements data are recorded in the control box. The control box also makes the calculations for determining PAI. Usually the below records consist of multiple measurements to obtain a spatial average [Welles and Norman, 1991].

4.5.2. Indirect measurements of the biomass by LAI-2000 PCA

In this study the attempt was made to estimate the AGB by an optical sensor. The projected area of the above-ground biomass (AGB) is captured by the sensor, and may correlate with the AGB. For this purpose the optical sensor LAI-2000 PCA was used. The projected area of stem, branches and leaves is called the plant area index (PAI). For the total plant area index, an effective PAI must be divided by the clumping factor; hence the LAI-2000 PCA determines a realistic effective plant area index (PAI_e) [Privette et al., 2004]. For simplification, the traditional notations of the obtained output by LAI-2000 PCA were converted into plant area index (PAI), plant area density (PD) and drip line plant area index (DLPAI) instead of leaf area index (LAI), foliage density (PD) and drip line leaf area index (DLLAI). There may be a measurable relationship between the projected area and AGB, if the biomass (stem and branch) is considered as cylindrical body and the cross-section surface is observed by the optical sensor. At regular time intervals, the effective plant area index of five woody species was measured with the LAI-2000 PCA using the one sensor mode. In order to identify the most suitable approach in using the LAI-2000 PCA device on individual woody species, four different methods were applied and compared with destructive sampling to find the best fit between the destructive method and LAI-2000 PCA measurements. The optical sensor required the path lengths through the canopy to calculate the average value according to the five viewing angles of different observed canopy volumes. The default set up for the path lengths was either defined by one divided by cosine (angle) for each viewing angle, or by a distance vector which was determined by measuring two canopy radii at a right angle to each other and canopy height. The average value of these three values was entered as distance vector, accordingly the same average distance value for each of the five view angles was defined. Entering the distance values were generally directly conducted to the control box.

As a result, the LAI-2000 PCA device

was either set up to $1/\cos$ (angles) or the path lengths for each view angle were labeled as a distance vector. A further modification was the position of the sensor. In the case of trees the



Fig. 7. Canopy structure considered from the bottom to the top

sensor was placed centrally below the canopy: for bush types central on the soil or at midpoint between center and outer edge for trees and under bushes at the underside of the canopy. The combinations of these two settings produced four methods.

With the sensor position at half distance between center and outer edge, the sensor viewing range was directed towards the center. The sequence of the above and below records was set to one above reading and eight below readings. One exception to the above sensor viewing range was the tree type which was measured locally and centrally on the underside of the canopy outset. The sequence for the tree species was one above reading alternating with one below reading with eight replications. Hence the canopies of the trees with this position of the sensor were measured in angles of 90° around the tree trunk, using the 90° view cap. The other methods were generally measured with the 270° view cap. If this view cap was not suitable, either because of surrounding interference factors, such as other shrubs and trees located too close to the examined species, or because of difficult weather conditions like fast changing cloudiness degree, or the need for measurements towards the sun, view caps with more limited visual range were applied and documented.

Table 2. Field set-up and position modifications of the four methods.

method	path lengths		position sensor	
	1/cos (viewing angles)	DISTS-Vector	Centrum	midpoint
1	x		x	
2	x			x
3		x	x	
4		x		x

The degree of cloudiness that prevailed during the measurements was separately noted when measuring above the stock and, once, for measuring below the stock, and were distinguished between cloudless sky and cloudy sky. However, when the above reading was taken under sunny conditions and the below reading was performed under cloudy circumstances, both files were later coded as measurements under cloudy conditions and vice versa.

4.5.3. Software FV2000 for further processing of the acquired field data

The software FV2000 was used for further processing of the raw data from the LAI-2000 PCA. The records were transformed from the default set up, to skip repetitions of a below record when transmittance values exceeded the corresponding reference values by the previously measured above reading, and to maintain all repetitions. The measured transmittance in each ring of the below record was divided by transmittance in each ring of the above record, and, if the below reading ring transmittance was higher, the ring(s) was/were set to 1 and the remaining rings were used for the calculation. For the previous set up, in which one was divided by cosines for each viewing ring and was set up in the control box on the field for two of the four methods, corrected path lengths through the shrub and tree individuals were calculated with the canopy model called “Isolated Canopy-Computed Distances” (manual FV2000). This canopy model required the entering of the vertical profiles of each species repetition, therefore vertical profiles were created with the help of a meter rod. The profiles were drawn into a coordinate system. The other canopy model is called “Isolated Canopy-Measured Distances” and constitutes the setup of the other two methods wherein a distance vector was determined. Entering the distance values was generally directly conducted to the control box in the field.

Table 3. Summary of the modifications in the field and the further handling of the software application FV2000.

growing form	method	field				FV2000
		path lengths	position of the sensor at the underside of the canopy	cap		
bush	1	1/cos	center	90°	VP	
	2	1/cos	midpoint between center and outer edge	90°	VP	
	3	DISTS	center	90°	-	
	4	DISTS	midpoint between center and outer edge	90°	-	
tree	1	1/cos	center	270°	VP	
	2	1/cos	midpoint between center and outer edge	90°	VP	
	3	DISTS	center	270°	-	
	4	DISTS	midpoint between center and outer edge	90°	-	

The Horizontal Uniform canopy model derived path lengths from the function one divided by cosines of the angles. If the path lengths differ from these function results, the LAI values were not interpreted as PAI ($\text{m}^2 \text{m}^{-2}$), but the obtained LAI-2000 PCA values were expressed as PD ($\text{m}^2 \text{m}^{-3}$). To convert PAI ($\text{m}^2 \text{m}^{-2}$) into PD ($\text{m}^2 \text{m}^{-3}$) the PAI value must be divided by the canopy height (manual FV2000). This applies to the implementation of the horizontal uniform model, for example, homogeneous and large plant communities. However, with regard to the heterogeneous savanna plant communities and the isolated trees, the LAI-2000 PCA Index depends both on ground position, and on the corresponding associated ground size (manual LAI-2000). For this reason PD was converted into DLPAI; hence a change in the ground position did not alter the size of LAI-2000 PCA values and the defining of a specific area resulted in a clear determination of PAI.

4.5.4. Projection to the bottom

For method 1 and 2, the conversion into DLPAI was automatically provided by the FV2000 software which utilizes the vertical profile to calculate plant volume and canopy area. The other two methods with DISTS do not include the calculation into DLPAI. For method 3

and 4, three different kinds of conversion PD into DLPAI were tried. The first try was the

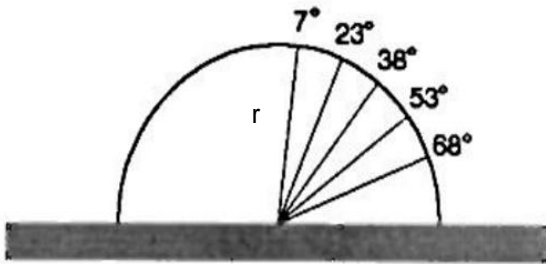


Fig. 8. Illustrates the DIST vector in the side view with the 5 viewing angles and the shape which defines a spatial hemisphere (modified after manual LAI-2000).

conversion with a canopy structure like a hemisphere. The vector spans a hemisphere with the radius (r), hence the distance through the canopy for each viewing angle is called DIST vector (Fig. 8). The volume and the projection area were calculated for each individual repetition of the measured species.

The second try was the conversion of PD into DLPAI by using the volume and the

projected area of an ellipsoid form - an ellipsoid form is the most common form to describe plant canopy. The volume and the projected area to the bottom were calculated for each tree and bush on each of the twelve plots which are divided into four different vegetation types.

$$V = \frac{2}{3}\pi r^3$$

$$A = \pi ab$$

a, b = ellipse half-axis

a, b, c = ellipsoid half-axis

The ratios were set in relation to the total height of the respective tree or bush. The received equations by plotting for each species were used to receive the conversion factor for each individual repetition of the measured species by insertion of the individual canopy height. The same conversion factors obtained from the vertical profile by method 1 and method 2 were used for the third conversion with the function of control and better evaluation.

4.5.5. Determination of the AGB by optical based method

All three plots with the size 30 * 30 meters for the four different vegetation types were outlined in the soil with boundary markers. Each plot was cataloged in the year 2012. The starting point and two perpendicular angled lines fixing the frame of each plot were pointed

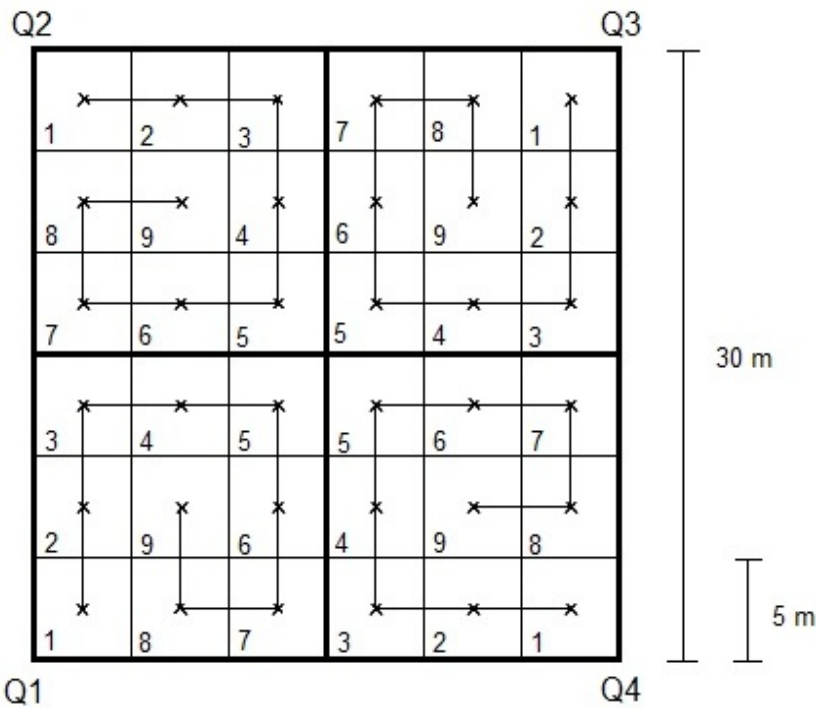


Fig. 9. Chart of travel paths for the measurements with the LAI-2000 PCA.

out by the needle of a compass. The installation was done with the help of two tape measures, at first arranged on the vertical lines and marked from 2.5 m at intervals of 5 meters up to 30 m. Then one tape was displaced parallel to the endpoint of the other vertical line, readjusted, and also marked at the distance of 5 m.

Subsequently the other tape, still lying on the original line, was shifted on both sides to the nearest marker point, and in succession to the next ones. Wooden sticks were hammered into the soil at an interval of 5 m and at a distance of 2.5 m from the plot border marker point. The plot was divided into four major squares (Q1, Q2, Q3 and Q4) and each major square was further subdivided into nine subplots. This subdivision resulted into 36 subplots with the lengths of 5 * 5 m, and with one permanently installed marker in the midpoint. At each corner point of the mayor squares, one above reading and then nine below readings was made so that at each installed marker point of the nine subplots of the major square one below reading was ensured. The direction of the track along the marker points was kept clockwise. The measured view field of the sensor for each reading was directed and adjusted to the center of the plot.

At each corner point of the mayor squares, one above reading into the middle point of the whole plot was made and nine below readings, so that at each installed marker point of the nine subplots in the mayor square was ensured.

The viewing direction of the optical sensor was always into the center of the plot. LAI-2000 PCA measurements were carried out, for the three bush-tree-savanna plots (BT1, BT4 and BT5), on which both the destructive and non-destructive measurements took place, and, with also high frequency, for the three grass savanna plots (G1, G5 and G7). The frequency for the three bush plots (B1, B2 and B5) and the three tree savanna plots (T2, T3 and T5) was lower. Missing values were sorted out; measurement values of zeros were included for the calculation of the average carbon density on plot-level.

4.6. Statistical Analyses

Statistical analyses were performed by using SPSS Statistics, version 22. The samples were independent in regard to the different points in time of harvesting. Within the points in time the samples of the different species were completely randomized. A general linear model (LM) was conducted to determine if the separated plant compartments in the volume, like biomass or leaf area, differ over species and time. However, after the data set was transformed, the inspection of sample distribution by box plot identified no outliers or extreme values. Above ground biomass values were approximately normal-distributed. Although, on the third time point of harvest, *A. bussei* was not normal-distributed, this result was neglected due to the fact that a non parametric test showed that the factor time of harvest for *A. bussei* was not significant. For all factor combinations the values were normal-distributed, as assessed by Shapiro-Wilk's test ($p > 0.05$). There was homogeneity of variances, as assessed by Levene's Test of Homogeneity of Variance ($p > 0.05$, $p = 0.054$).

The model for the AGB was defined as:

$$y = \mu + \textit{species} + \textit{time point} + \textit{species} * \textit{time point}$$

The volumetric leaf area was also normal-distributed for all group combinations of species and for time. The homogeneity of variances was tested by Levene's Test of Homogeneity of Variances ($p > 0.05$, $p = 0.061$). There was a significant interaction term between the two factors, therefore it was necessary to change the syntax in SPSS to determine the differences between species at each harvest date and vice-versa. The model equation was equal. For the DLPAI, outliers and extreme values were removed from the LAI-2000 PCA dataset because with high probability the outliers and extreme values were due to measurement errors of the in-field-device (e.g. pollution of the lens). Boxplots were used for identifying outliers and extreme values. For statistical analyses, the two datasets were combined to one dataset. The dates of destructive harvesting were shifted to the nearest time of non-destructive measurements and linked with the destructive measured values. Normal-distribution and variance homogeneity were often not met for the individual purposes. The attempt was to confirm normal-distribution by Log transformation and Box Cox Transformation, and it seemed as if common assumption was better reached by natural logarithm transformation. Non-parametric tests (e.g. Kruskal Wallis) depend on similar shape distribution to identify differences between the groups, but also the SD vary widely, hence only mean ranks and not

median values of the species should be compared. LAI-2000 PCA measurements values were repeated measurements and not independent in time and also not balanced between each time point of the repeated measurement. The frequently repeated measuring of different subjects (e.g. species) is the reason for the heteroscedasticity [e.g. Wolfinger, 1996; Fortin et al., 2007], and, in my opinion, non normal-distribution of the data was a cluster effect of species. Despite the fact that assumptions were not met, an univariate general linear model was used for this purpose. The first model was:

$$\text{AGB} = \text{intercept} + \text{species} + \text{method} + \text{DLPAI} + \text{species} * \text{DLPAI}$$

The second model for the species was:

$$\text{AGB} = \text{intercept} + \text{species} + \text{DLPAI} + \text{species} * \text{DLPAI}$$

The studentized residual were plotted in histogram. The data showed an approximately normal-distribution, and parameter estimation for regression lines were similar with the estimations of robust/non-linear or generalized linear models (glm included the possibility to deal with unbalanced repeated measurements).

5. Results

5.1. Destructive Methods

5.1.1. Canopy density of the species

The species canopy density (CD; kg m^{-3}) was measured by destructive method. Fig. 10 shows the results: the CD (kg m^{-3}) amounted to 2.66 (± 0.63), 3.97 (± 1.05), 2.07 (± 0.33), 4.37 (± 1.41), and 6.40 (± 1.52) for five different species: *A. bussei*, *A. nilotica*, *A. nubica*, *A. tortilis*, and *Achyr. aspera*, respectively.

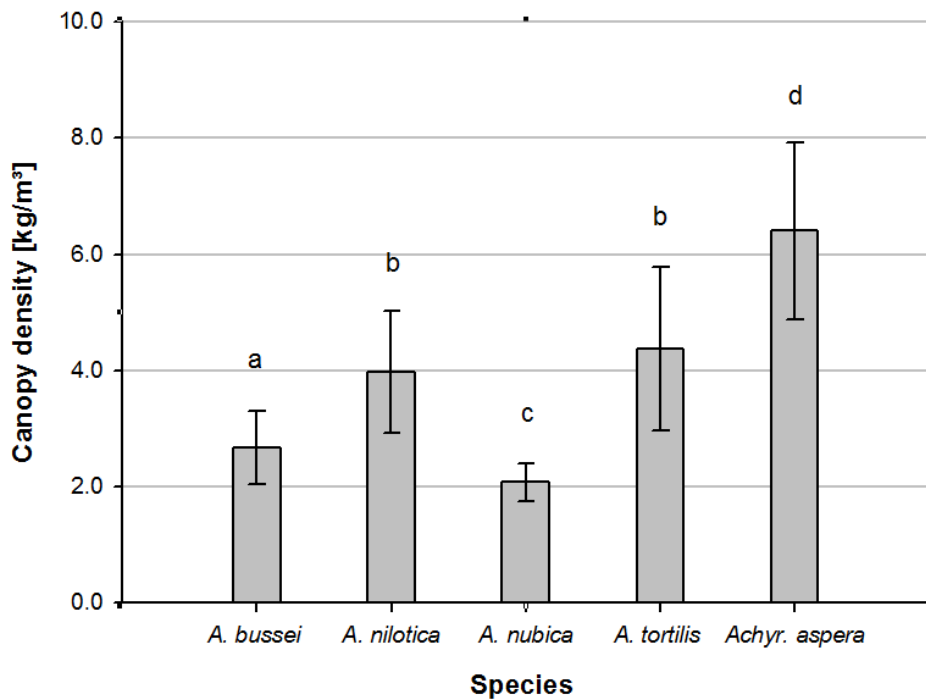


Fig. 10. Canopy density [kg m^{-3} ; mean, \pm standard deviation] of the examined species. Mean values followed by the same letters are statistically not significantly different [$p < 0.05$].

There was no statistically significant difference ($p = 0.935$) in the above-ground biomass per volume (kg m^{-3}) between the different times of harvesting, but highly significant differences ($p < 0.0005$) could be observed between the species. The determined CD (kg m^{-3}) was statistically not significantly different between the two tree species *A. nilotica* and *A. tortilis* ($p < 0.05$)

5.1.2. Specific leaf area values of the species

Leaf area- and mass values were used to determine species-specific leaf area (SLA; $\text{m}^2 \text{kg}^{-1}$). The development of leaf area is shown in the next figure (Fig. 11). The SLA ($\text{m}^2 \text{kg}^{-1}$) is similar to each other, with 7.15 (± 1.11) for *A. bussei*, 8.37 (± 1.16) for *A. nubica*, and 8.19 (± 1.07) for *Achyr. aspera*. Lower SLA values ($\text{m}^2 \text{kg}^{-1}$) were reached by the species *A. nilotica* with 4.56 (± 0.57) and by *A. tortilis* with 5.37 (± 0.94). There were significant differences ($p < 0.05$) between these two groups.

Table 4. Specific leaf area values of the different species and the relevant statistical analysis; SD = standard derivation; rep. = repetitions.

species	SLA	SD	rep.
<i>A. bussei</i>	7.15 ^a	± 1.11	n = 9
<i>A. nilotica</i>	4.56 ^b	± 0.57	n = 6
<i>A. nubica</i>	8.37 ^a	± 1.16	n = 10
<i>A. tortilis</i>	5.37 ^b	± 0.94	n = 7
<i>Achyr. aspera</i>	8.19 ^a	± 1.07	n = 7

5.1.3. Leaf area density

During the rainy season, the leaf area density (LD; $\text{m}^2 \text{m}^{-3}$), also harvest destructively of five species, was very variable and depended on the harvest time point (2-weeks interval) and on the species (Fig.11). The change of LD ($\text{m}^2 \text{m}^{-3}$) was also different within a species - compared to the LD ($\text{m}^2 \text{m}^{-3}$) of other species over the vegetation season. The averaged leaf biomass per canopy volume (kg m^{-3}) in relation to biomass per canopy volume (kg m^{-3}) amounted to 0.124 kg m^{-3} (4.66 %) for *A. bussei*, 0.413 kg m^{-3} (10.37 %) for *A. nilotica*, 0.105 kg m^{-3} (5.05 %) for *A. nubica*, 0.250 kg m^{-3} (5.71 %) for *A. tortilis*, and 0.187 kg m^{-3} (2.87 %) for *Achyr. aspera*.

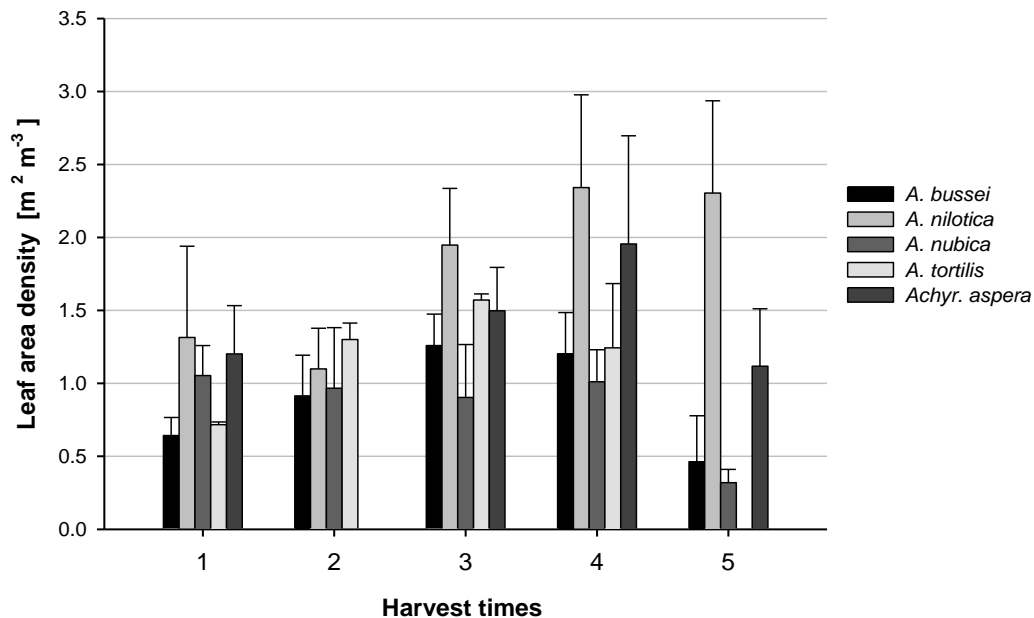


Fig. 11. Change in leaf area density [$\text{m}^2 \text{m}^{-3}$; means; \pm standard deviation] during a rainy season [Nov. - Jan.] in Borana Zone, Ethiopia. The time period between each destructive harvest was about two weeks.

Statistical differences were observed in the LD ($\text{m}^2 \text{m}^{-3}$) between the species at the third date of harvest ($p = 0.026$), and highly significant differences were observed in the leaf area per canopy volume ($\text{m}^2 \text{m}^{-3}$) between the species at the fourth date of harvest ($p = 0.001$), and fifth date of harvest ($p < 0.0005$). At the third harvest, *A. nilotica* and *A. nubica* were statistically different ($p < 0.05$) in their LD ($\text{m}^2 \text{m}^{-3}$). At the next harvest date, not only statistical differences ($p < 0.05$) in LD ($\text{m}^2 \text{m}^{-3}$) between *A. nilotica* and *A. nubica* were measured, but also statistical differences in LD ($\text{m}^2 \text{m}^{-3}$) between *A. nilotica* and *A. bussei* and

also between *A. nilotica* and *A. tortilis* were found. In addition to the fourth harvest, the last harvest showed significant differences in LD ($\text{m}^2 \text{m}^{-3}$) between *Achyr. aspera* and the other species. There were no significant differences ($p = 0.074$) measured for the leaf area ($\text{m}^2 \text{m}^{-3}$) of *Achyr. aspera* during the whole growing season. No statistical differences were found in the mean leaf area ($\text{m}^2 \text{m}^{-3}$) on the first, the second, and the last harvest date - despite an increase in the volumetric leaf area ($\text{m}^2 \text{m}^{-3}$) of *A. nilotica* compared to the LD ($\text{m}^2 \text{m}^{-3}$) of the other Acacia species at the end of the rainy season.

5.2. Non-destructive Methods´

5.2.1. Relationship of species-specific plant area density as measured by LAI-2000 PCA

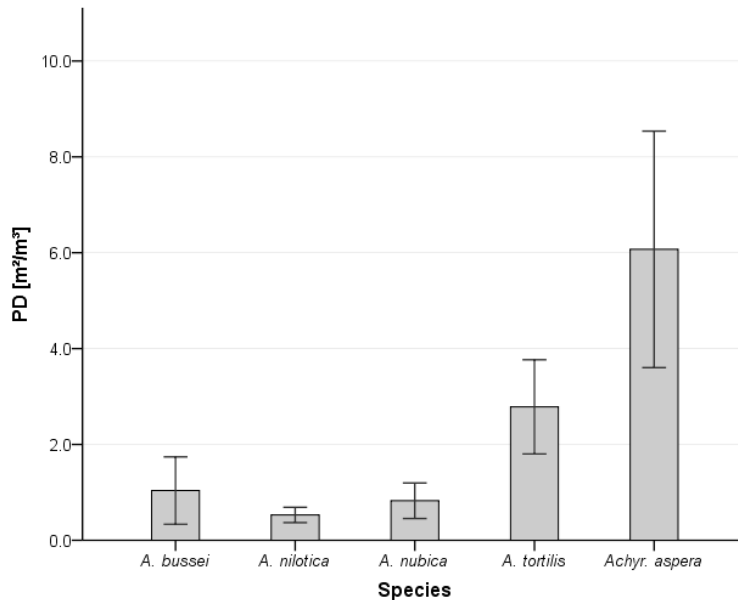


Fig. 12. Species-specific plant area density [FD = m² m⁻³; means, ±SD; all LAI-2000 PCA Plant Canopy Analyzer measurement values were used for calculation].

The average values of the plant density values (PD; m² m⁻³) were 1.04 (±0.70) for *A. bussei* (median value = 0.76), 0.53 (±0.16) for *A. nilotica*, 0.83 (±0.37) for *A. nubica* (median value = 0.78), 2.79 (±0.98) for *A. tortilis*, and 6.07 (±2.47) for *Achyr. aspera*. Taking the PD values into consideration, no clear result could be found. The assumption of normal-distribution and variance homogeneity was not met for each group. Although some subset transformation with natural logarithm resulted in normal-distribution, nevertheless, significance tests showed different results for each subset, obtained by the use of Games Howell Post Hoc Test for unequal variances and sample size. The assumed results of a non-parametric test were also not met because the Kruskal-Wallis Test is sensitive to heterogeneous variances [Lix et al., 1996]. There is no statistical evidence that *A. tortilis* and *Achyr. aspera* share the same PD (m² m⁻³). However, looking at the descriptive results, the standard deviation (SD) of *Achyr. aspera* was high, and the real median value may be in the same range as *A. tortilis*. In contrast, *A. nilotica*, *A. bussei* and *A. nubica* reached lower values. In all the tests these three species were always

significantly different to *A. tortilis* and *Achyr. aspera*. Within these two groups different tests showed no clear pattern and depended on the choice of the sub-sample.

5.2.2. The compare of canopy density to plant area density for each species

Within the species there was a high variability in both plant area density (PD $\text{m}^2 \text{m}^{-3}$) and destructive harvest canopy density (CD; kg m^{-3}).

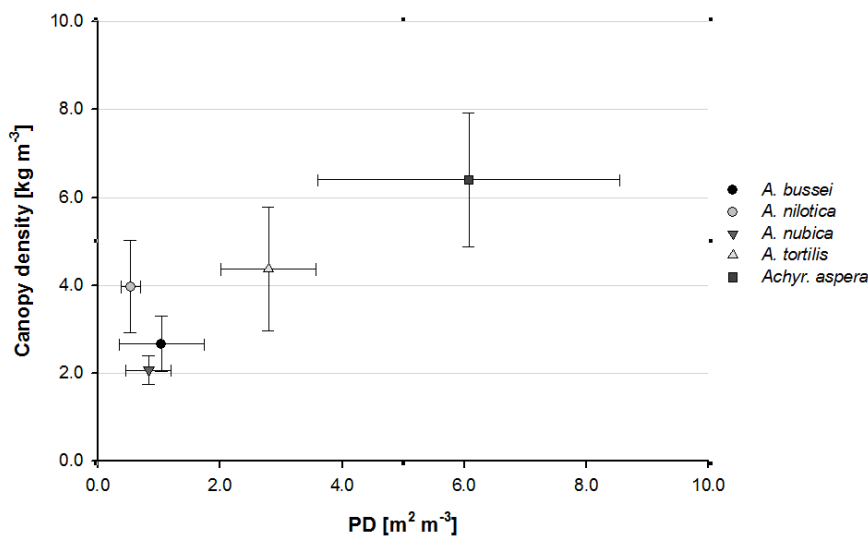


Fig. 13. Species-specific plant area density [PD = $\text{m}^2 \text{m}^{-3}$; means, \pm SD] to species-specific canopy density [CD = kg m^{-3} ; means, \pm SD]. All measurement values were used.

Taking the median into consideration, it becomes obvious that *A. bussei* is similar to both *A. nilotica* and *A. nubica*. However, *A. nubica* and *A. nilotica* appear to be different, and, likewise, PD ($\text{m}^2 \text{m}^{-3}$) measurement values resulted in different CDs. Increase in PD for *A. tortilis* and *Achyr. aspera* led to higher CD (kg m^{-3}). The averaged PD ($\text{m}^2 \text{m}^{-3}$) of *A. tortilis* and a SD multiplied by one resulted in a PD ($\text{m}^2 \text{m}^{-3}$) value on the left side of 3.60. Mean value of *Achyr. aspera* multiplied by one SD ranged up to 3.57 on the right side; hence there is no overlapping range of the distributions. It should be noted that normal-distribution was not reached in all groups, because most of the species would be equal under normal-distribution and ± 1.96 SD, that is 95 % confidence interval.

5.2.3. Destructive and non-destructive measurements of canopy density and area

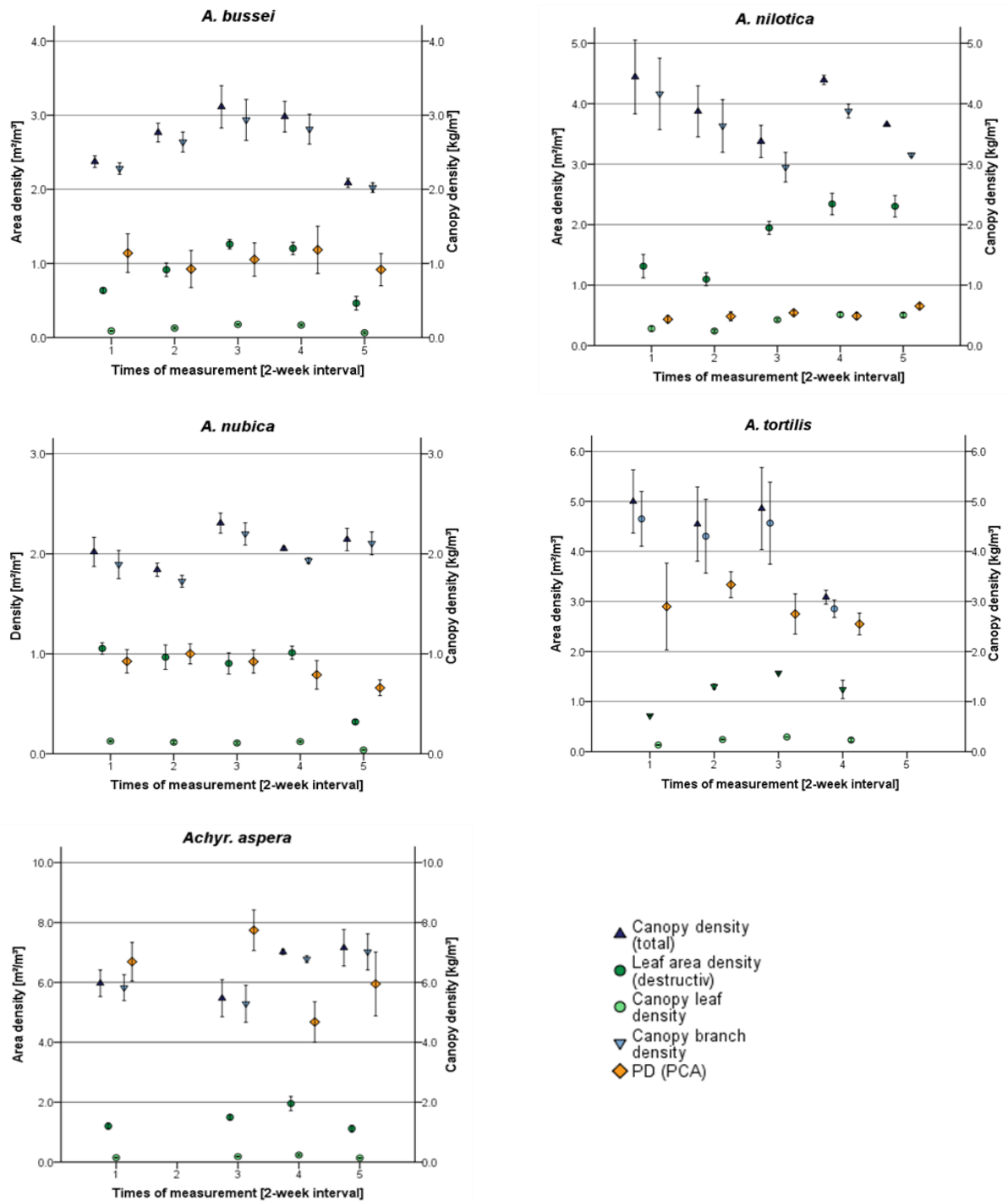


Fig. 14. Destructive and non-destructive measurements over the trail time. LAI-2000 Plant Canopy Analyzer measured the plant area density [PD = m² m⁻³].

During the considered time period, the quantity (Fig. 14) of both destructive measured values and non-destructive measured PD ($\text{m}^2 \text{m}^{-3}$) values was, over the observed period, on the same level, and even parallel in most of the cases. *A. nilotica* had the highest amount of leaf biomass per one cubic meter; PD values ($\text{m}^2 \text{m}^{-3}$) were lower than the leaf area density measured by destructive method. For the alteration of the destructive leaf density and PD ($\text{m}^2 \text{m}^{-3}$) over the time no statement was possible. The alteration of leaf area during the season was correlated to the LAI-2000 PCA measured values. The change in leaf biomass was low in the observed time frame. If present, the measurement errors of the LAI-2000 PCA outweighed the change of leaf area density.

5.2.4. Influence of wood density and leafs to the optical measured total plant area

The correlation between stem area index and biomass depended on the different wood density of the species. In literature, the wood densities values were not found for all species. Considering pooled data for species composition, species with higher wood density are underestimated. Wood density is 800 kg m^{-3} for *A. nilotica*⁴, whereas *A. bussei* is a heavy wood and, with its oven-dried density of 928 kg m^{-3} , it is used for charcoal production⁵. In a study about the potential of biomass for energy production, a density of 461 kg m^{-3} was observed for the bush type species *Achyr. aspera* [Subramanian and Sampathrajan, 1990].

In the observed period the change in leaf biomass was low. If present, the measurement errors of the LAI-2000 PCA outweighed the change of leaf area density. However, statistical analyses resulted in a significant relationship between PD ($\text{m}^2 \text{m}^{-3}$) and destructive measured LD ($\text{m}^2 \text{m}^{-3}$). The adj. r amounted to 0.444.

It seems possible that for some species both canopy density (kg m^{-3}) and leaf area density ($\text{m}^2 \text{m}^{-3}$) derive from the optical measured area density ($\text{m}^2 \text{m}^{-3}$). In two cases the increase in measured PD was positively correlated to LD ($\text{m}^2 \text{m}^{-3}$): for *A. nilotica* ($p < 0.0005$) and for *A. nubica* ($p = 0.030$). For the other species of the evaluation process, the leaf area showed no significant effect on the measured PD ($\text{m}^2 \text{m}^{-3}$).

⁴FAO, (1997). Estimating Biomass and Biomass Change of Tropical Forests.

⁵FAO, (1987). Simple technologies for charcoal making.

5.2.5. Summary (1)

The consideration of the destructive and non-destructive values showed that

1. The canopy density of *A. nilotica* and *A. tortilis* reached the same high canopy density values, however, *Achyr. aspera* had the highest values. Moreover, between *A. nilotica* and *A. tortilis* the specific leaf area was not significantly different.
2. LAI-2000 PCA measurements showed that *A. bussei*, *A. nubica* and *A. nilotica* are similar in plant area density. However, *A. nilotica* reached the lowest values.
3. *A. nilotica* had the highest leaf biomass.

5.2.6. Pooled data

The next figure shows the relationship between CD (canopy density; destructive; kg m^{-3}) and PD (plant area density; non-destructive; $\text{m}^2 \text{m}^{-3}$) for the pooled data. The outliers were removed by the use of 95% confidence interval of an additionally y-value. The residual were approximately normal-distributed, if PD ($\text{m}^2 \text{m}^{-3}$) was transformed by natural logarithm. The use of measurements under cloudy sky resulted in $r^2 = 0.585$ and measurement values under sunny condition reached $r^2 = 0.301$. Although twice as many records with the LAI-2000 PCA were made under sunny conditions, than under cloudy sky, no significant difference between cloudy and sunny conditions have been observed.

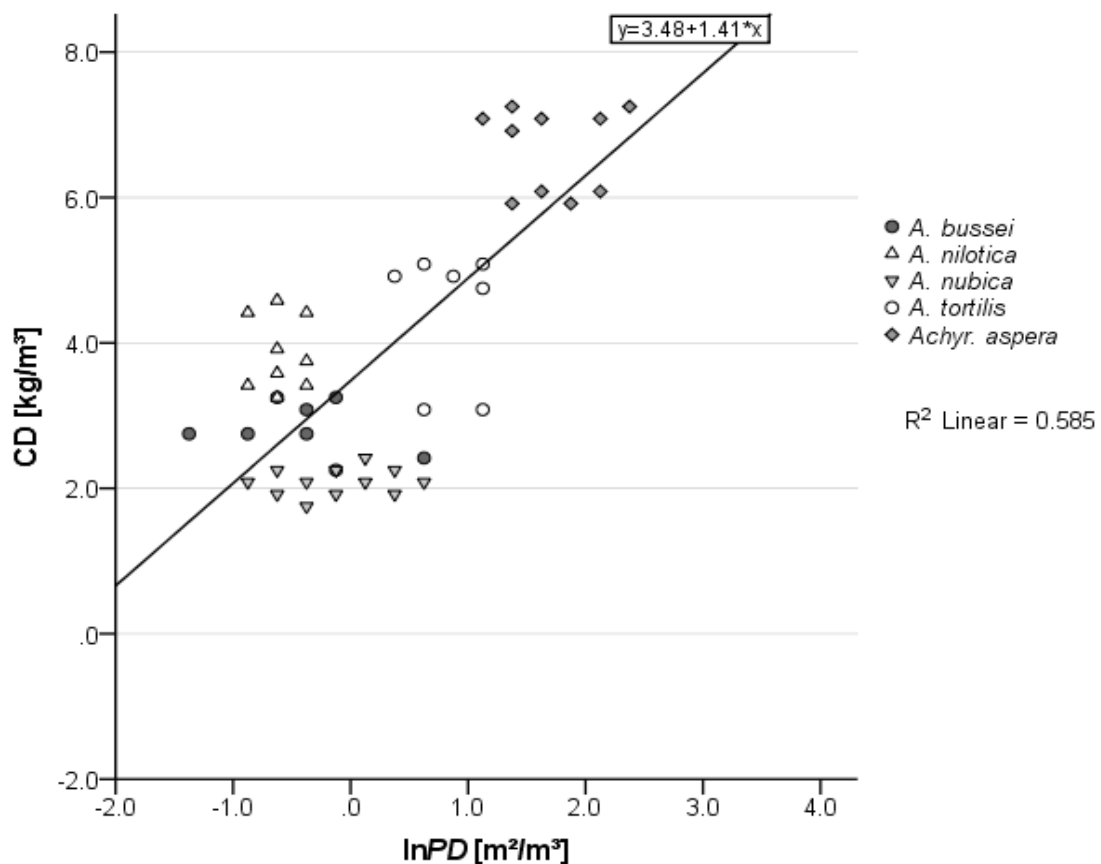


Fig. 15. Regression line of canopy density [CD, mean values of each harvesting; PD (transformed by natural logarithm), measurement values; CD = kg m^{-3} , PD = $\text{m}^2 \text{m}^{-3}$; outliers were removed by 95% confidence interval; only measurement values under cloudy condition were used].

The CD (kg m^{-3}) is related nonlinear to PD ($\text{m}^2 \text{m}^{-3}$). Hangs et al. [2011] measured with the LAI-2000 PCA the stem area index of willows. This study also found a non-linearity relationship between SAI and AGB. The increase in above-ground biomass resulted in an

increase of volume, but, in contrast, the cross section area measured by the optical sensor increased not with the same factor. The increase was proportional to $r \sim V^2$. In this case the different wood densities of the species additionally may have had an effect on the observed non-linearity.

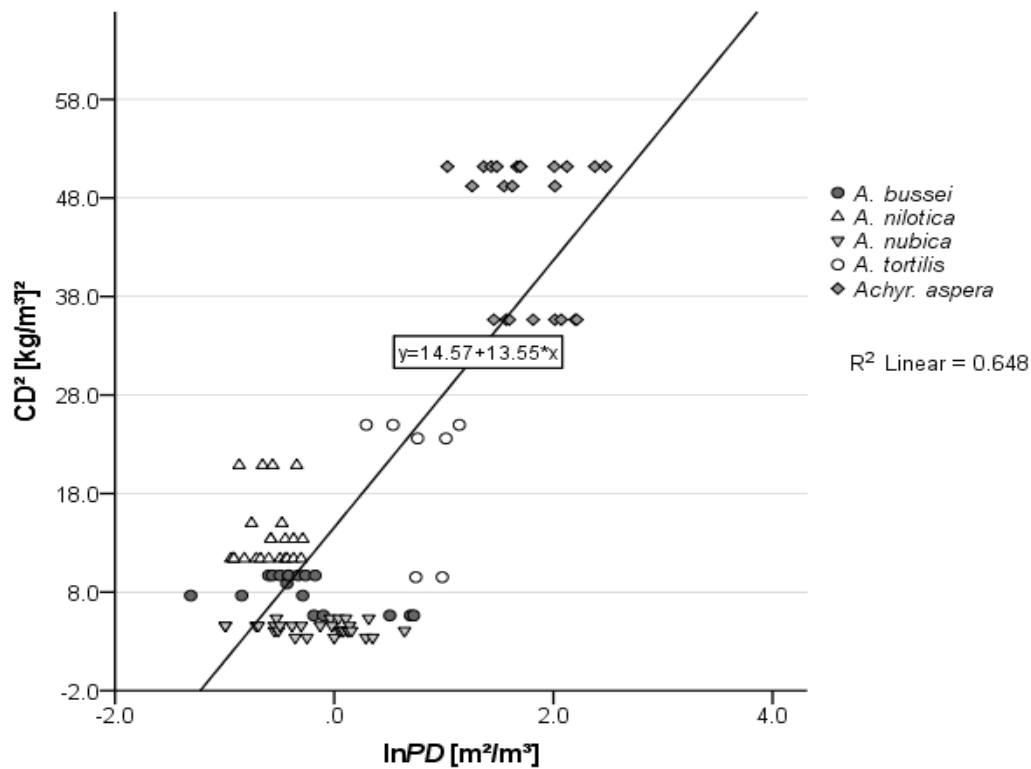


Fig. 16. Regression line for squared canopy density [CD, mean values of each harvesting; PD (transformed by natural logarithm), measurement values; CD = kg m^{-3} , PD = $\text{m}^2 \text{m}^{-3}$; outliers were removed by 95% confidence interval; only measurement values under cloudy condition were used].

The determination of correlation r^2 increased from 0.585 to 0.648 for CD (kg m^{-3}) and CD^2 (kg m^{-3})², respectively. The relationship between CD or CD^2 and transformed PD ($\text{m}^2 \text{m}^{-3}$) was significant ($p < 0.05$).

5.3. Species-specific Above-ground Biomass Estimation

5.3.1. Methods comparison

For the detail consideration of the species, measured values of the repetitions of each species were converted from PD ($\text{m}^2 \text{m}^{-3}$) into DLPAI ($\text{m}^2 \text{m}^{-2}$). Canopy density (kg m^{-3}) too was converted into above-ground biomass (AGB; kg m^{-2}) by the same conversion factor. The figures of each species for each method and conversion factor can be found in the appendix.

For method 3 and 4 different methods were applied to obtain conversion factors. (Method 1 and 2 conversion factors were calculated by software FV2000). The first subset was the conversion of PD ($\text{m}^2 \text{m}^{-3}$) into DLPAI ($\text{m}^2 \text{m}^{-2}$) using a hemisphere for the shape of the canopy. The results showed that there was a significant relationship between DLPAI ($\text{m}^2 \text{m}^{-2}$) and AGB (kg m^{-2}); the different species, the species-specific increase in measured DLPAI to AGB, and the different methods were significant ($p < 0.05$). Detail consideration of methods 3 and 4 showed that statistically they were significantly different compared to method 1 and 2, whereas with the measurement values of method 3 ($p = 0.664$) and 4 ($p = 0.087$) the relationships between DLPAI ($\text{m}^2 \text{m}^{-2}$) and AGB (kg m^{-2}) were not significant, the results showed no significant differences between the slopes of the different methods - with the exception of *A. nubica*, which is a quite uniform bush; hence all methods obtained the same results. The method of measuring should not influence the estimation of above ground biomass; hence a hemisphere may not be the appropriate geometrical form to describe the shape of an uniform shrub and, especially, not the shape of tree canopies. For that reason an ellipsoid form for the shape of the canopy was applied. Once the canopy shape was considered as an ellipsoid, the comparative analyses of the four methods showed no significant differences between the examined methods for the different species. Equal could be noticed when the same conversion factors, obtained from the vertical profiles (manual FV2000) for method 1 and 2, were also used for method 3 and 4 to convert PD ($\text{m}^2 \text{m}^{-3}$) into DLPAI ($\text{m}^2 \text{m}^{-2}$). The use of the same conversion factors improved the adjusted coefficient of determination from $\text{adj. } r^2 = 0.704$ to $\text{adj. } r^2 = 0.740$ because the data of the methods converged.

The conversion factors obtained by the vertical profile were used for further analyses for the species, and the term method was removed from the model equation. The harvest time was not significant ($p = 0.865$). The relationship between DLPAI ($\text{m}^2 \text{m}^{-2}$) and AGB (kg m^{-2}) was

significant at $p < 0.05$. The AGB (kg m^{-2}) was significantly different between the species ($p < 0.5$), and there was a significant interaction between DLPAI ($\text{m}^2 \text{m}^{-2}$) and species ($p = 0.001$). The adj. r^2 was 0.745.

5.3.2. The comparison of the different species

The pairwise comparison of the estimated marginal means adjusted by the mean values of the covariate (DLPAI) indicated that *Achyr. aspera*, *A. nubica*, and *A. tortilis* are not significantly different from each other. *A. bussei* and *A. nilotica* are significantly different to each of the other species. Significant differences in the slope were found by comparing the regression lines of *A. nilotica* and *Achyr. aspera*, also the differences in the intercept values were significant ($p < 0.05$) to each of the other species. *A. bussei* had a significantly different slope to *A. nubica*, *A. tortilis* and *Achyr. aspera*, but the difference in slope to *A. nilotica* was not significant ($p = 0.09$).

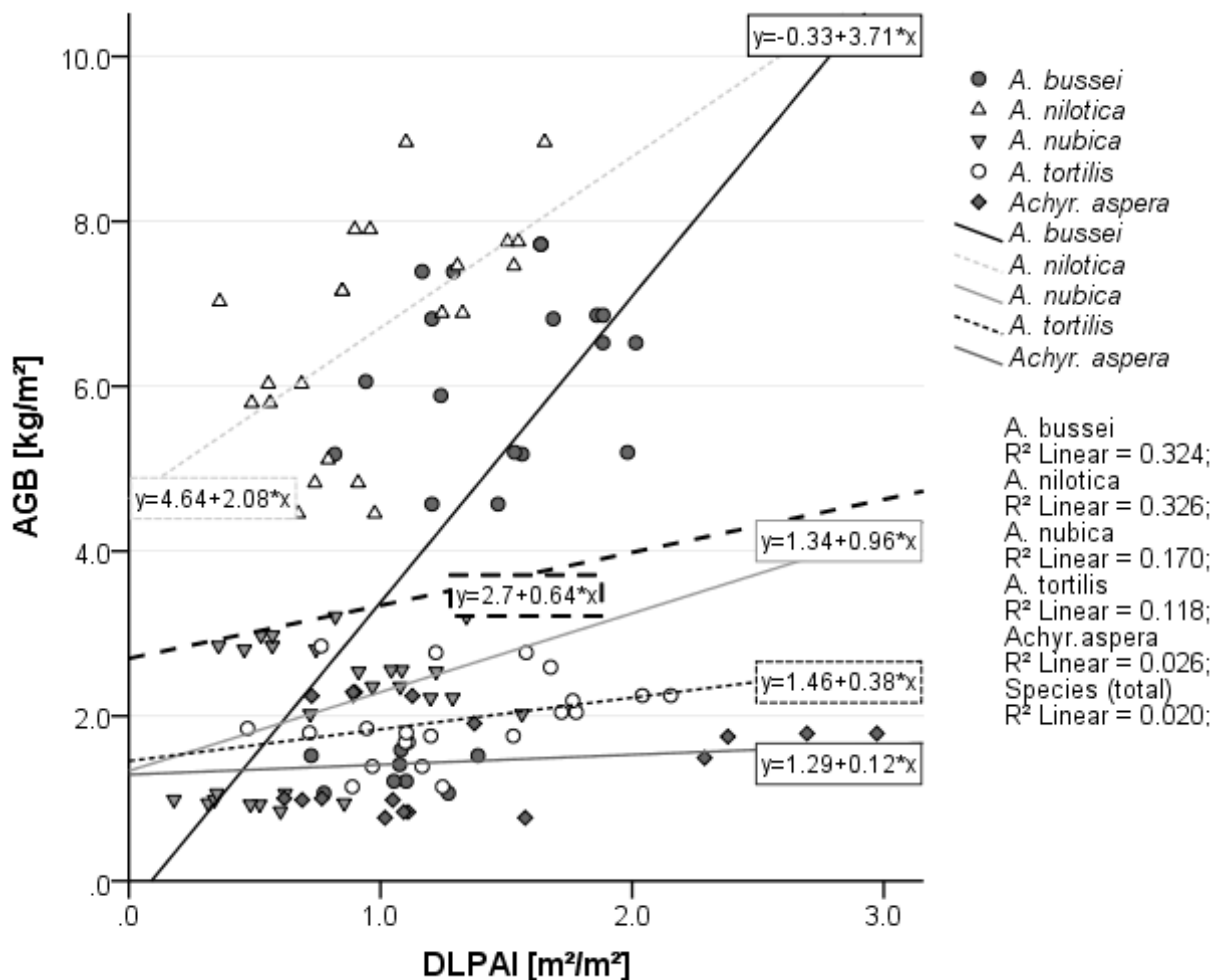


Fig. 17. Species specific regression lines of AGB [AGB, mean values of each harvesting and species repetition; DLPAI, measurement values; AGB = kg m⁻², DLPAI = m² m⁻²; outliers were removed by 95% confidence interval].

For the pooled data, the relationship between DLPAI (m² m⁻²) and AGB (kg m⁻²) was not significant ($p < 0.113$; adj. $r^2 = 0.011$; $n = 115$). Examined tree sizes of the three non-

destructive measured samples were very similar to *A. nilotica*, while the tree sample sizes of *A. bussei* were widely spread. The regression line of *A. bussei* had the steepest slope and the deepest intersection point (0.0,-0.33). In contrast, the regression line of *A. nilotica* intersected the y-axis at 4.64; therefore displaying the highest intercept.

5.3.3. Influence of increasing leaf area on the above-ground biomass

The following figure (Fig. 18) shows the studentized residual correlated to destructive measured leaf area. Increasing leaf area resulted in a positive residual. Taking the intercept into view, the straight lines intersected the y-axis in the negative range, and the slopes were positive. This suggests that an underestimation of observed AGB (kg m^{-2}) occurs for lower values of leaf area, and vice versa. Overestimation of the observed AGB (kg m^{-2}) occurred for higher values of leaf area.

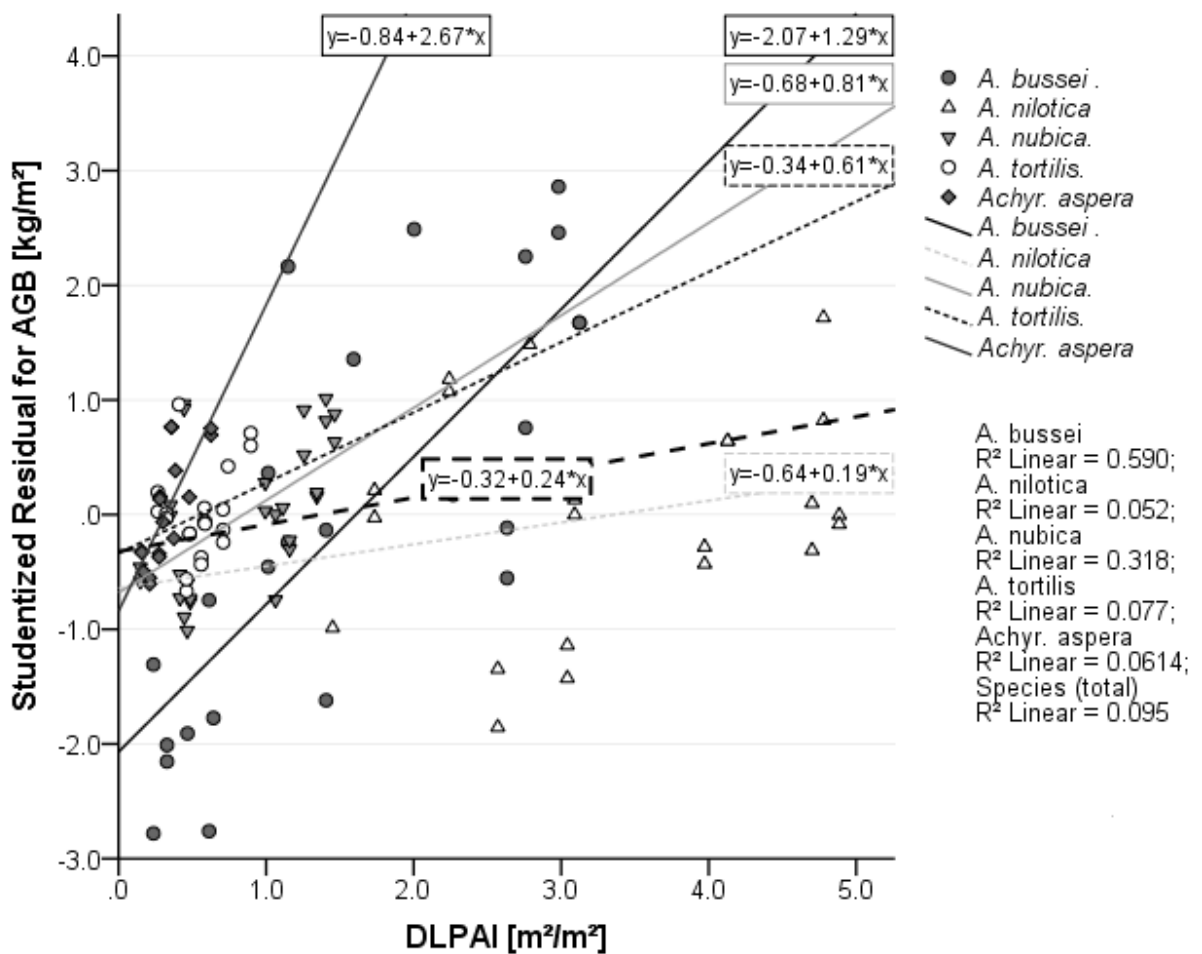


Fig. 18. Plot of studentized residual obtained from regression analyses versus increasing leaf area [$\text{m}^2 \text{m}^{-2}$].

There was lesser interest in leaf biomass because most of the carbon remained bound only for a short-time due to e.g. leaf shedding.

5.3.4. Summary (2)

1. The comparison of the canopy density and of the plant density showed a relationship between canopy density and increasing PD. The ratio between canopy density and plant area density for the different species was not the same.
2. The detailed consideration of each species inverted the expected values. The regression lines of each species, with regard to the canopy volume and crown area, shifted. The low PD which was converted into DLPAI values did result in high biomass amounts per crown area.

5.4. Consideration of the Canopy Structure

5.4.1. Ratio of canopy density to plant area density

The next figure (Fig. 19) shows PD ($\text{m}^2 \text{m}^{-3}$) values and the ratio of CD (kg m^{-3}) to PD ($\text{m}^2 \text{m}^{-3}$). The data transformation with natural logarithm was the most appropriate transformation in this data set, that is the antiderivative of $f(x) = 1/x$.

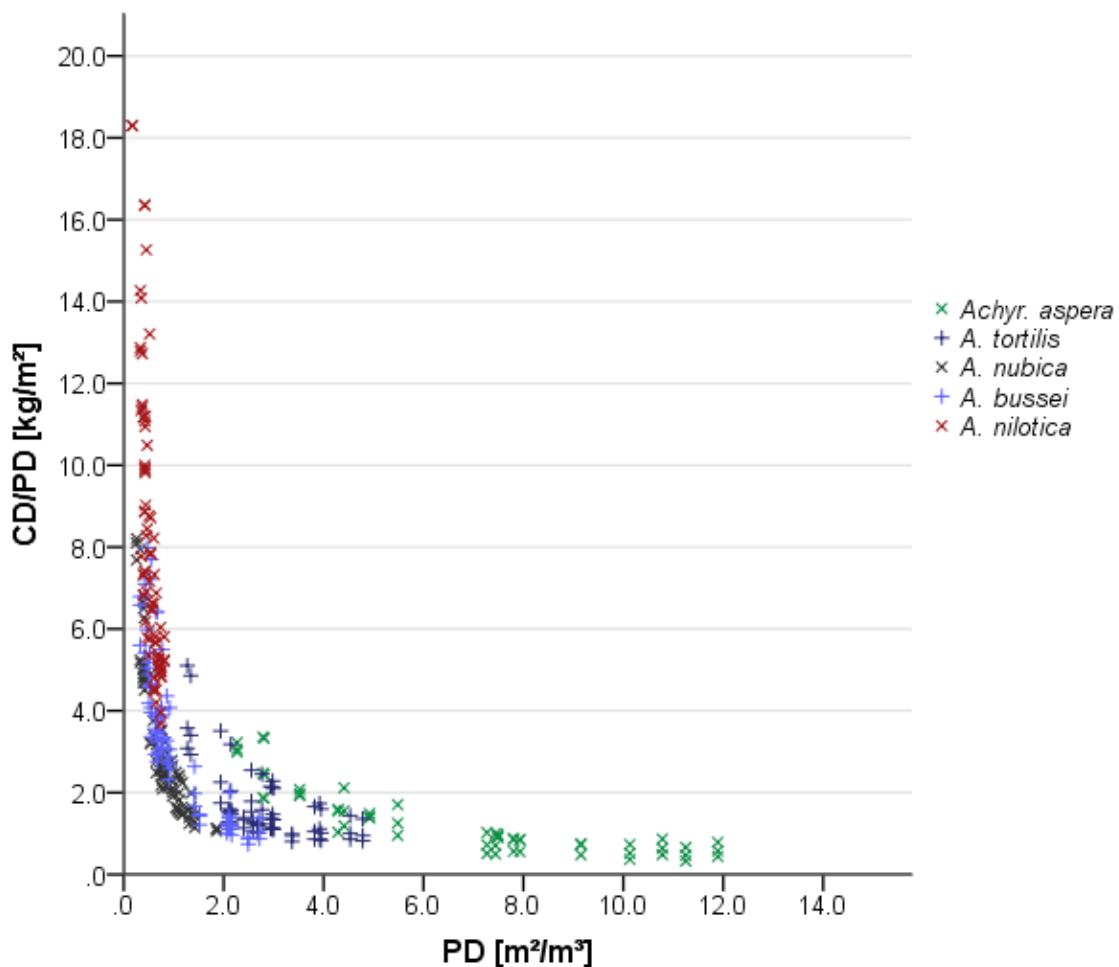


Fig. 19. The ratio of canopy density [CD; kg m^{-3}] to plant area density [PD; $\text{m}^2 \text{m}^{-3}$] in comparison to the increasing PD [$\text{m}^2 \text{m}^{-3}$].

In proportion, low measurement values resulted in higher canopy density (kg m^{-3}) if compared to higher measured PD values ($\text{m}^2 \text{m}^{-3}$) obtained by LAI-2000 PCA. The different species seemed to merge into one another. *A. tortilis*, *A. bussei* and *A. nubica* were spatially closer together, whereas measured in terms of distances each of the two species *A. nilotica* and

Achyr. aspera were farther away from the other. The ratio of canopy density (kg m^{-3}) to PD ($\text{m}^2 \text{m}^{-3}$) seemed to be overestimated for the lower values and underestimated for the higher values of PD ($\text{m}^2 \text{m}^{-3}$), or, otherwise, PD ($\text{m}^2 \text{m}^{-3}$) was underestimated for *A. nilotica* and overestimated for *Achyr. aspera*. The same pattern could be observed for the ratio of leaf area to PD ($\text{m}^2 \text{m}^{-3}$). The examined values were transformed with natural logarithm. Because no values existed for *A. tortilis*, measurement values of method 3 and 4 were sorted out. The examination by post-hoc test for unequal variances showed that the ratio of canopy density (kg m^{-3}) to PD ($\text{m}^2 \text{m}^{-3}$) was not significantly different for *A. bussei* and *A. nubica*. The non-parametric test was less vulnerable to outliers and, therefore, no significant differences between *Achyr. aspera* and *A. tortilis* were observed too.

5.4.1. Species-specific clumping index

Clumping index was calculated by destructive measurements. Destructive woody biomass was separated between smaller samples and samples larger than 1 cm in stem diameter. The Stem area index was corrected by wood density (kg m^{-3}). The clumping index of each species and repetition resulted in the conclusion that with increasing ratio of canopy volume to area, which is correlated to tree height, the clumping effect decreased. This result might be a special case because the smaller species were underestimated and, additionally, this false impression was boosted by high measurement values in the field. Taller species reached higher clumping index values, hence these species were less underestimated - although more biomass was considered by the sensor. Also the underestimation of the species by LAI-2000 PCA depended on their size and on their canopy structure.

Table 5. Summarized clumping effect of each species; clumping effect was calculated by destructive samples.

species	rep. no.	crown area [m ²]	crown volume [m ³]	LAI _d [m ² m ⁻²]	SAI _d [m ² m ⁻²]	DLPAl _{eff} [m ² m ⁻²]	DLPAl [m ² m ⁻²]	Ω	tree height [m]
<i>A. bussei</i>	1	0.24	0.47	1.76	2.33	1.02	4.09	0.249	1.4
<i>A. bussei</i>	2	14.58	5.88	0.36	0.48	1.37	0.84	1.625	5
<i>A. bussei</i>	3	10.43	4.76	0.41	0.54	1.68	0.95	1.761	4.3
<i>A. nilotica</i>	1	9.94	7.55	1.37	0.93	0.65	2.29	0.283	4.5
<i>A. nilotica</i>	2	12.67	6.2	0.88	0.60	1.24	1.48	0.839	6.5
<i>A. nilotica</i>	3	14.56	6.86	0.85	0.57	0.96	1.42	0.675	5.2
<i>A. nubica</i>	1	1.53	1.39	0.77	1.18	1.13	1.95	0.579	2.25
<i>A. nubica</i>	2	5.86	4.22	0.61	0.94	0.74	1.55	0.478	3.5
<i>A. nubica</i>	3	0.36	0.76	1.79	2.74	0.46	4.54	0.101	0.8
<i>A. tortilis</i>	1	4.38	11.7	3.23	3.61	0.9	6.84	0.132	5.5
<i>A. tortilis</i>	2	5.96	10.47	2.13	2.37	1.34	4.50	0.298	6.8
<i>A. tortilis</i>	3	2.8	6.19	2.67	2.98	1.75	5.66	0.309	3.3
<i>Achyr. aspera</i>	1	0.06	0.19	4.56	6.65	1.37	11.21	0.122	0.55
<i>Achyr. aspera</i>	2	0.02	0.14	10.08	14.70	0.91	24.78	0.037	0.35
<i>Achyr. aspera</i>	3	0.02	0.08	5.76	8.40	2.12	14.16	0.150	0.5

5.4.2. Estimation of spatial carbon density distribution on plot level

Modifications for estimation of carbon density on plot level were made. Grass savanna and its above-ground biomass amount were lower than the biomass amount of woody species. Therefore, to obtain a full data range, the biomass and LAI-2000 PCA values had to be included into the regression line. For that reason, a few grass plots were measured not only destructively, but also by the LAI-2000 PCA. With the destructive method the SLA of grass amounted to approximately $0.6 \text{ (m}^2 \text{ kg}^{-1}\text{)}$. The destructive sample size of species in the grass savanna was lower than the sample size of woody species. The implementation of the measurement values into the regression line of CD (kg m^{-3}) with PD ($\text{m}^2 \text{ m}^{-3}$) observed no realistic slope, therefore all measured values of LAI-2000 PCA were used and, subsequently, the regression line was shifted through the origin. The determined slope parameter was 1.056. This parameter was reached by a Bootstrap- regression, and the same parameter was also obtained by the ordinary least squares (OLS) method. The second modification was the consideration of the different mean canopy heights, because with increasing canopy height the volume of the hemispheric view increased more than the correlated projected area at the bottom. The factor of the second conversion was $2/3$ multiplied by the mean canopy height. The correlation between carbon content and vegetation type was tested by Spearman's rho and this correlation was significant ($p < 0.01$).

Results on plot level showed that there were significant differences in carbon content between the different vegetation types (VT).

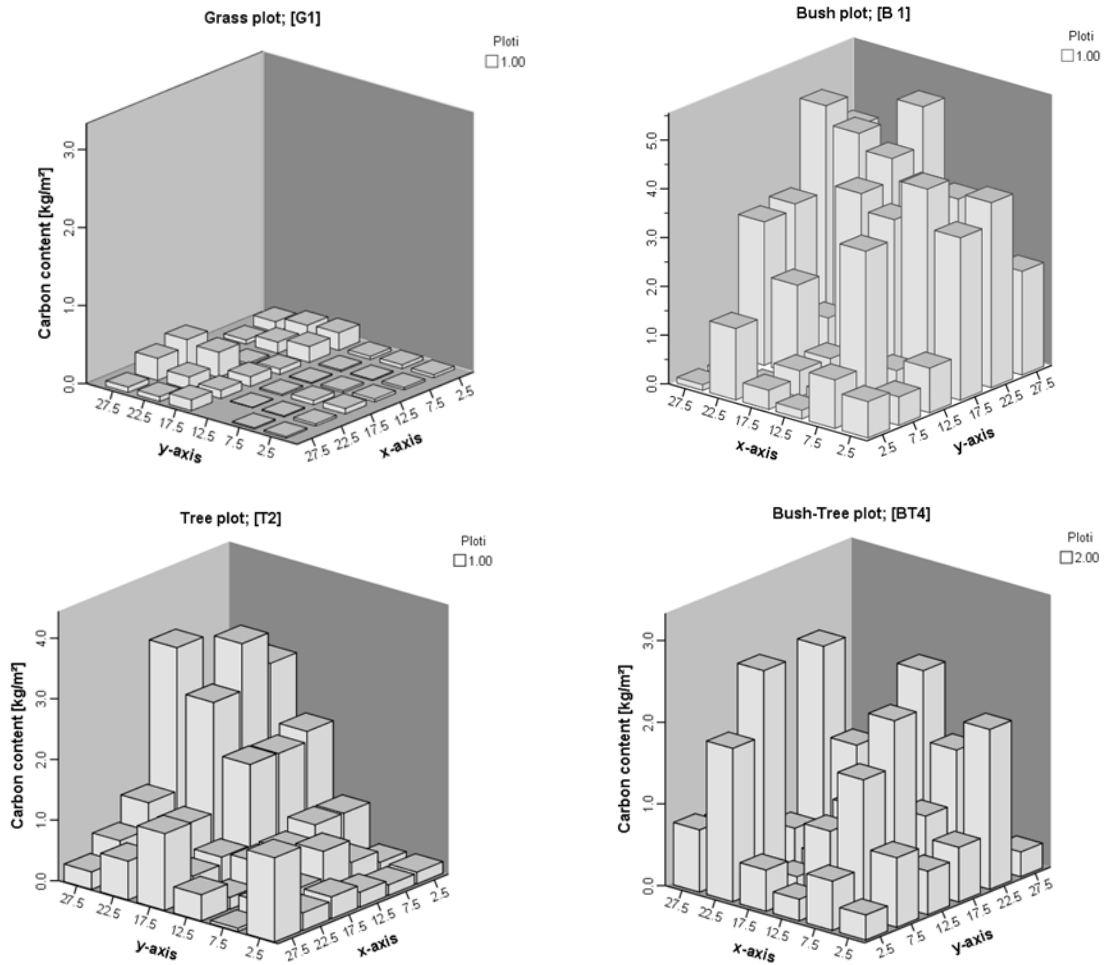


Fig. 20. Carbon content for each grid point; illustrated is one plot of each vegetation type [mean values; kg m⁻²]

The data was not normal-distributed because both, the comparison test of Games Howell and the non-parametric test were used, and both tests showed the same results. The above-ground biomass (kg m⁻²) for the different VT amounted to 3.2 for bush-savanna (B), 3.7 to tree-savanna (T), 2.71 for bush-tree-savanna (BT), and 0.26 for grass-savanna (G). No significant differences in estimated carbon content (kg m⁻²) were observed, neither between bush-tree- and bush-savannas, nor between tree- and bush-savannas. The conversion of biomass into carbon content was 50% [e.g. Houghton et al., 2009].

5.4.3. Summary (3)

1. The observed canopy density to plant area density decreased with a higher plant area density.
2. The calculation of the clumping index showed the exact size of underestimation ($\Omega < 1$) and overestimation ($\Omega > 1$) of each species repetition.
3. The underestimation of the different species and their repetitions may depend on different factors (e.g. growing form or species size).
4. The Calculation of the clumping index allowed for the possibility to draw conclusions about the source of errors. The high bias (, that is to say the distortion of results,) was due to the modifications which have been made there, together with the special environmental conditions in comparison to the common measurements with the LAI-2000 PCA.

6. Discussion

This paper's comparisons of the different methods showed that the conversion received from the ratio of volume to area by a hemispherical form is not the appropriate geometrical form to describe the non-uniform shape of a shrub - or even to describe the shape of tree canopies. The most common form to describe a plant canopy is an ellipsoid form. Working with the DISTs vector is coarser, but requires less effort, because neither the determination of the vertical profile in the field, nor the consideration of the vertical profile and recalculation of the path lengths in respect for each individual species are required. The obtained foliage density values obtained by the simplification, attained with the DISTs vector, should subsequently be converted into DLPAI through the use by an ellipsoid form.

The influence of the existence of leaves was for two examined species significant, but reached a negligible effect for three of the five species and it may have a higher effect than here observed on the measured values by the LAI-2000 PCA, because, after the rainy season, leaf shedding was neither observed for *A. nilotica*, nor for *A. tortilis*. Furthermore, the starting point of the main experiment was not early enough in time to capture the whole leaf development. All species had already developed leaves. The result that plant area density is a good predictor for both; canopy density and leaf area density is similar to the result that the canopy volume of shrubs is a good predictor for above-ground biomass and for foliage biomass in allometric equations. If the leaf area has an effect on LAI-2000 PCA measurements, then self-shading and leaf angle are influencing the amount of light capture within a species, even if the quantity of leaves during a vegetation period is low. The leaf angle changes not only in relation to the sun position [Falster and Wetoby, 2003], but also with increasing aridity [Scholes et al., 2004].

A. tortilis increases root growth by osmotic adjustment in the root-zone as a strategy to postponement dehydration [Otieno et al., 2001]. This results in later leaf shedding. Likewise, *A. nilotica* is shown to be a drought resistant species which exhibits several drought avoiding adaption responses, such as an increase of root:shoot ratio under drought conditions [Michelsen and Rosendahl, 1990]. A study on adaption mechanisms to drought of different bush and tree species in the savanna of Ethiopia reported higher growth rates for species with mechanisms for avoiding drought [Gebrekirstos et al., 2006]. The subjective observations on the species compositions indicated that the observed encroacher species mainly used the

avoiding mechanism and shed their leaves early as response to drought [Oldeland et al., 2010]. Therefore, the encroachment species seemed to have a better productivity, which resulted in a higher carbon sequestration potential. In the study of [Oldeland et al., 2010], encroacher species were detected by remote sensing methods. Due to the fact of leaf shedding and less understory vegetation, the soil led to a change in the obtained signal. The later leaf shedding species *A. tortilis* also occurred as an encroachment species; *A. tortilis* had the most pronounced thorn structure of all examined species. Thorny species were observed to have a selective advantage compared to non-thorny species due to lesser browsing pressure [Moleele et al., 2002].

Aref and El-Juhany [2004] reported that SLA ($\text{m}^2 \text{kg}^{-1}$) of *A. tortilis* decreased by 10.32 $\text{m}^2 \text{kg}^{-1}$ to 2.43 $\text{m}^2 \text{kg}^{-1}$ under drought stress. *A. tortilis* also showed the lowest SLA values, compared to other Acacias [Aref and El-Juhany, 2004]. In our study, the SLA ($\text{m}^2 \text{kg}^{-1}$) of *A. tortilis* also belonged to the species with the comparatively smaller SLA values ($\text{m}^2 \text{kg}^{-1}$). Additionally, *A. mellifera*, a species that forms fine leaves that are similar structured to that of the examined species, is also occurring in the research area and also an encroacher was shown to reach SLA values of up to 5.52 $\text{m}^2 \text{kg}^{-1}$ [Scholes et al., 2004].

In comparison to the other three species *A. nilotica* and *Achyr. aspera* were not collected under the same spatial conditions. This resulted in spatial heterogeneity but different encroacher species often occur not under the same spatial conditions [Oldeland et al., 2010], so maybe the different areas are not important and even a typical aspect. Still the measurement values of *A. nilotica* were the lowest of all species; *A. nilotica* is growing very isolated without surrounding trees. The effects of the surrounding landscape, together with the different canopy structure, may be higher than the measurement of the species itself. However, the field of view of the sensor is very wide and can capture the canopy in a radius of e.g. 14.8 m for a averaged canopy height of six meters. Hence, the measured values of the species with more surrounding trees and bushes partially include a background noise.

The required assumptions for measuring with the LAI-2000 PCA are: a) the examined object is a black body b) the distribution of the leaves in space is random c) the distance between the object and the sensor must be large enough, and d) the orientation of the object is azimuthal and random (manual LAI-2000). The results of measurements with the LAI-2000 PCA on plot level showed that the highest values measured were found for the Bush savanna. This is mainly due to the fact that the distance between the bushes and the optical sensor was close to each other. Increasing distance between sensor and object under investigation results in an

underestimation because the percentage of plant area to the total viewing area decreases. In this study, the sensor position was always hold at canopy start level, but it would have been useful to make reference records in different heights under the canopy start for each of the species too.

Scholes et al. [2004] also measured the effective plant area index with the LAI-2000 PCA in savannas along a moisture gradient. For shrubland and fine leafed savanna the reported values were between 1.75 ($\text{m}^2 \text{m}^{-2}$) and 0.78 ($\text{m}^2 \text{m}^{-2}$). Plant area index was also measured with the Accupar sensor, a sensor for Photosynthetically Active Radiation (PAR). The position of the Accupar sensor was at 1 m height, and the position of LAI-2000 PCA at approximately soil surface. LAI-2000 PCA readings were lower compared to the readings of the Accupar sensor, although the field of view of optical sensor of the LAI-2000 PCA captures more canopies. In the Shrub savanna, Scholes et al. [2004] also reported comparatively high LAI-2000 PCA readings and reasoned that LAI-2000 PCA values depend on canopy height. These results are similar compared to our results.

Ryu et al [2010] measured with different instruments and approached an element clumping index for leaf area index determination. Also conducted in a savanna, the measurements led to the conclusion that the open structure and the canopy shape have beneficial effects on the measurements with the LAI-2000 PCA. The decrease in the clumping index enhances the clumping effect because the LAI-2000 PCA values are divided by the index, and, consequently, the underestimation of the projected area to the sensor rises. In this study, no significant effect of zenith angles on the measurements could be observed. The different wood densities of the species could also be neglegate. The small variations in the density resulted in even more smaller size alteration of the observed cross section area, indicated that the species are very similar to each other, but the canopy architecture has an effect on the LAI-2000 PCA measurements [Sampson, 1995]. The comparison of the remote sensing results with the clumping index in this study showed that our results are in the same range [Hill et al, 2003] and the in this study not significant effect of the weather conditions was really differently than expected and could be an effect of the canopy structure.

Not included for the use of the LAI-2000 PCA device is the fraction of litter lying on the ground surface and measurement with the LAI-2000 PCA on plot level at soil surface includes the grass layer, but the LAI of the grass layer is combined with low biomass amounts therefore, contingently, two regression lines are required for the measurements on plot level.

7. Conclusion

Not only measurements of the species should be converted into DLPAI, but also, since all differences in the estimated parameters, which may have influenced the measurements, arise mainly from different clumping indexes, more measurements must be conducted to estimate the effect of clumping for each of the different parameters. In my opinion, the number of repetitions sampled for each species was not enough. As a result, and the clumping index indicate the high underestimation for smaller bushes (e.g. *A. bussei*; repetition number 1) the resulting slope of the linear regression was too steep. Apparently, plants out of the Acacia species appeared quiet similar - although the respective measurements taken with the LAI-2000 PCA showed high differences.

I suggest that on plot level the different clumping indexes measured for the different plants and species resulted in an average ecosystem clumping index of about 0.5 because this is a value that corresponds well with estimations for the same parameter measured via remote sensing methods for the same area. Overall, it seems to be possible to measure the biomass with this device. However, the estimation of the biomass with the LAI-2000 PCA needs further examination, but for the time being the examined method seems to be efficient and fast, and this is the most significant feature that is needed to estimate the potential in carbon sequestration by wood encroachment.

References

Angassa, A., Tolera, A., and Belayneh, A., (2006). The effects of physical environment on the condition of rangelands in Borana. *Tropical Grasslands*, 40, 33–39.

Angassa, A., (published online: 2012). Effects of grazing intensity and bush encroachment on herbaceous species and rangeland condition in southern Ethiopia. *Land Degradation and Development*.

Angassa, A., and Oba, G., (2013). Cattle herd vulnerability to rainfall variability: responses to two management scenarios in southern Ethiopia. *Tropical Animal Health and Production*, 45(3), 715–721.

Aref, I.M., and El-Juhany, L.I., (2004). Effects of drought stress on the growth of *Acacia asak* (Forssk.), *A. tortilis* (Forssk.) and *A. gerrardii* (Benth) ssp. *negevensis* (Zoh.). *Monsura university Journal of Agricultural Sciences*, 24(10), 5627–5636.

Asner, G.P., Archer, S., Hughes, R.F., Ansley, R.J., and Wessman, C.A., (2003). Net changes in regional woody vegetation cover and carbon storage in Texas Drylands, 1937–1999. *Global Change Biology*, 9, 316–335.

Baccini, A., Laporte, N., Goetz, S. J., Sun, M., and Dong, H., (2008). A first map of tropical Africa's above-ground biomass derived from satellite imagery. *Environmental Research Letters*, 3(4).

Bala, G., Devaraju, N., Chaturvedi, R.K., Caldeira, K., and Nemani, R., (2013). Nitrogen deposition: how important is it for global terrestrial carbon uptake? *Biogeosciences*, 10, 7147–7160.

Global Energy Assessment: Toward a Sustainable Future. Banerjee, R., Benson, S.M., Bouille, D.H., Brew-Hammond, A., Cherp, A., Coelho, S.T., Emberson, L., Figueroa, M.J., Grubler, A., Jaccard, M., Ribeiro, S.K., Karekezi, S., He, K., Larson, E.D., Li, Z., McDade, S., Mytelka, L.K., Pachauri, S., Patwardhan, A., Riahi, K., Rockström, J., Rogner, H.-H., Roy, J., Schock, R.N., Sims, R., Smith, K.R., Turkenburg, W.C., Ürge-Vorsatz, D., von Hippel, F., and Yeager, K., (2012). Cambridge University Press, Cambridge, UK and New York, NY, USA and the International Institute for Applied Systems Analysis, Laxenburg, Austria.

Beltràn-Przekurat, A., Pielke Sr., R.A., Peters, D.P.C., Snyder, K.A., and Rango, A., (2008). Modeling the effects of historical vegetation change on near-surface atmosphere in the northern Chihuahuan Desert. *Journal of Arid Environments*, 72(10), 1897–1910.

Breuer, B., (2012). Effects of vegetation type and species composition on carbon stocks in semi-arid Ethiopian savannas. M. Sc. Thesis, Universität Hohenheim, Stuttgart, Germany.

Blaum, N., Rossmannith, E., and Jeltsch, F., (2007). Land use affects rodent communities in Kalahari savannah rangelands. *African Journal of Ecology*, 45(2), 189–195.

Bockheim, J.G., and Gennadiyev, A.N., (2010). Soil-factorial models and earth-system science: A review. *Geoderma*, 159, 243–251.

Cao, M., and Woodward, F.I., (1998). Dynamic responses of terrestrial ecosystem carbon cycling to global climate change. *Nature*, 393.

Cissé, M.I., (1980). The browse production of some trees of the Sahel: Relationship between maximum foliage biomass and various physical parameters. *Le Houerou, H.N. (Ed.), Browse in Africa*, 205–210. ILCA, Addis Ababa, Ethiopia.

Claussen, M., Mysak, L.A., Weaver, A.J., Crucifix, M., Fichet, T., Loutre, M.-F., Weber, S.L., Aleamo, J., Alexeev, V.A., Berger, A., Calov, R., Canopolski, A., Goosse, H., Lohmann,

G., Lunkeit, F., Mokhov, I.I., Petoukhov, V., Stone, P., and Wang, Z., (2002). Earth system models of intermediate complexity: closing the gap in the spectrum of climate system models. *Climate Dynamics*, 18(7), 579–586

Collins, J.N., Hutley, L.B., Williams, R.J., Boggs, G., Bell, D., and Bartolo, R., (2009). Estimating landscape-scale vegetation carbon stocks using airborne multi-frequency polarimetric synthetic aperture radar (SAR) in the savannahs of north Australia. *International Journal of Remote Sensing*, 30(5), 1141–1159.

Coppock, D.L., (1993). Grass hay and Acacia fruits: A local feeding system for improved calf performance in semi-arid Ethiopia. *Tropical Animal Health and Production*, 25(1), 41–49.

Dalle, G., Maass, B.L., and Isselstein, J., (2006). Encroachment of woody plants and its impact on pastoral livestock production in the Borana lowlands, southern Oromia, Ethiopia. *African Journal of Ecology*, 44(2), 237–246.

Falster, D.S., and Westoby, M., (2003). Leaf size and angle vary widely across species: what consequences for light interception?. *New Phytologist*, 158(3), 509–525.

FAO, (1987). Simple technologies for charcoal making. (FAO Forestry Paper - 41), URL: <http://www.fao.org/docrep/x5328e/x5328e00.HTM>, (State: 04.08.2014).

FAO, (1997). Estimating Biomass and Biomass Change of Tropical Forests: a Primer. (FAO Forestry Paper - 134), URL: <http://www.fao.org/docrep/w4095e/w4095e00.HTM>, (State: 04.08.2014).

Fortin, M., Daigle, G., Ung, C.H., Bégin, J., and Archambault, L., (2007). A variance-covariance structure to take into account repeated measurements and heteroscedasticity in growth modeling. *European Journal of Forest Research*, 126(4), 573–585.

Franklin, J., and Hiernaux, P.H.Y., (1991). Estimating foliage and woody biomass in Sahelian and Sudanian woodlands using a remote sensing model. *International Journal of Remote Sensing*, 12(6), 1387–1404.

GEA, 2012: Global Energy Assessment – Toward a Sustainable Future. Cambridge University Press, Cambridge UK and New York, NY, USA and the International Institute for Applied Systems Analysis, Laxenburg, Austria.

Gebrekirostos, A., Teketay, D., Fetene, M., and Mitlöhner, R., (2006). Adaptation of five co-occurring tree and shrub species to water stress and its implication in restoration of degraded lands. *Forest Ecology and Management*, 229(1-3), 259–267.

Glatzle, S., (2012). Relationship between Vegetation type, soil type, soil moisture and carbon stocks in semiarid Ethiopian savannas. M. Sc. Thesis, Universität Hohenheim, Stuttgart, Germany.

Goetz, S.J., Baccini, A., Laporte, N.T., Johns, T., Walker, W., Kellndorfer, J., Houghton, R. A., and Sun, M., (2009). Mapping and monitoring carbon stocks with satellite observations: a comparison of methods. *Carbon balance and management*, 4(2).

Grace, J., Josè, J.S., Meir, P., Miranda, H.S., and Montes, R.A., (2006). Productivity and carbon fluxes of tropical savannas. *Journal of Biogeography*, 33, 387–400.

Haberl, H., Erb, K.H., Krausmann, F., Gaube, V., Bondeau, A., Plutzer, C., Gingrich, S., Lucht, W., and Fischer-Kowalski, M., (2007). Quantifying and mapping the human appropriation of net primary production in earth's terrestrial ecosystems. *PNAS*, 104(31), 12942–12947.

- Hairiah, K., Sitompul, S.M., van Noordwijk, M., and Palm, C.A., (2001). Methods for sampling carbon stocks above and below ground. International Centre for Research in Agroforestry (ICRAF), Bogor.
- Hangs, R.D., Van Rees, K.C.J., Schoenau, J.J., and Guo, X., (2011). A simple technique for estimating above-ground biomass in short-rotation willow plantations. *Biomass and Bioenergy*, 35(5), 2156–2162.
- Hasen-Yusuf, M., Treydte, A.C., Abule, E., and Sauerborn, J., (2013). Predicting aboveground biomass of woody encroacher species in semi-arid rangelands, Ethiopia. *Journal of Arid Environments*, 96, 64–72.
- Heimann, M., and Reichstein, M., (2008). Terrestrial ecosystem carbon dynamics and climate feedbacks. *Nature*, 451.
- Herrero, M., Thornton, P.K., Gerber, P., and Reid, R.S., (2009). Livestock, livelihoods and the environment: understanding the trade-offs. *Current Opinion in Environmental Sustainability* 2009, 1(2), 111–120.
- Hill, M.J., Román, M.O., Schaaf, C.B., Hutley, L., Brannstrom, C., Etter, A., and Hanan, N.P., (2011). Characterizing vegetation cover in global savannas with an annual foliage clumping index derived from the MODIS BRDF product. *Remote Sensing of Environment*, 115(8), 2008–2024.
- Houghton, R.A., (2003). Revised estimates of the annual net flux of carbon to the atmosphere from changes in land use and land management 1850–2000. *Tellus*, 55B, 378–390.
- Houghton, R.A., (2007). Balancing the global carbon budget. *Annual Review of Earth and Planetary Sciences*, 35, 313–347.

Houghton, R.A., Hall, F., and Goetz, S.J., (2009). Importance of biomass in the global carbon cycle. *Journal of Geophysical Research: Biogeosciences*, 114(G2).

IGBP terrestrial carbon working group (1998). The terrestrial carbon cycle: implications for the Kyoto Protocol. *Science*, 280(5368), 1393–1394.

Ingram, J.S.I., and Fernandes, E.C.M., (2001). Managing carbon sequestration in soils: concepts and terminology. *Agriculture, Ecosystems and Environment*, 87(1), 111–117.

IPCC, 2000: Special Report on Emissions Scenarios. Nakicenovic, N., Alcamo, J., Davis, G., de Vries, B., Fenhann, J., Gaffin, S., Gregory, K., Griibler, A., Jung, T.Y., Kram, T., Lebre La Rovere, E., Michaelis, L., Mori, S., Morita, T., Pepper, W., Pitcher, H., Price, L., Riahi, K., Roehrl, A., Rogner, H.-H., Sankovski, A., Schlesinger, M., Shukla, P., Smith, S., Swart, R., van Rooijen, S., Victor, N., and Dadi, Z., (2000). Cambridge University Press, Cambridge, United Kingdom and New York, NY, USA.

IPCC, 2006: IPCC Guidelines for National Greenhouse Gas Inventories. Prepared by the National Greenhouse Gas Inventories Programme. Eggleston, H.S., Buendia, L., Miwa, K., Ngara T., and Tanabe, K., eds., (2006). IGES, Japan.

IPCC, 2007: Climate Change 2007. The Physical Science Basis. Contribution of Working Group I to the Fourth Assessment Report of the Intergovernmental Panel on Climate Change. Denman, K.L., Brasseur, G., Chidthaisong, A., Ciais, P., Cox, P.M., Dickinson, R.E., Hauglustaine, D., Heinze, C., Holland, E., Jacob, D., Lohmann, U., Ramachandran, S., da Silva Dias, P.L., Wofsy S.C., and Zhang, X., (2007). *Couplings Between Changes in the Climate System and Biogeochemistry*. Cambridge University Press, Cambridge, United Kingdom and New York, NY, USA.

IPCC, 2007: Climate Change 2007. The Physical Science Basis. Contribution of Working Group I to the Fourth Assessment Report of the Intergovernmental Panel on Climate Change.

Solomon, S., Qin, D., Manning, M., Chen, Z., Marquis, M., Averyt, K.B., Tignor M., and Miller, H.L., eds., (2007). Cambridge University Press, Cambridge, United Kingdom and New York, NY, USA, pp. 996.

IPCC, 2013: Climate Change 2013. The Physical Science Basis. Contribution of Working Group I to the Fifth Assessment Report of the Intergovernmental Panel on Climate Change 2013. Bindoff, N.L., Stott, P.A., Achuta Rao, K.M., Allen, M.R., Gillett, N., Gutzler, D., Hansingo, K., Hegerl, G., Hu, Y., Jain, S., Mokhov, I.I., Overland, J., Perlwitz, J., Sebbari, R., and Zhang, X., (2013). *Detection and Attribution of Climate Change: from Global to Regional*. Cambridge University Press, Cambridge, United Kingdom and New York, NY, USA.

IPCC 2013: Climate Change 2013: The Physical Science Basis. Contribution of Working Group I to the Fifth Assessment Report of the Intergovernmental Panel on Climate Change. Christensen, J.H., Krishna Kumar, K., Aldrian, E., An, S.-I., Cavalcanti, I.F.A., de Castro, M., Dong, W., Goswami, P., Hall, A., Kanyanga, J.K., Kitoh, A., Kossin, J., Lau, N.-C., Renwick, J., Stephenson, D.B., Xie, S.-P., and Zhou, T., (2013). *Phenomena and their Relevance for Future Regional Climate Change*. Cambridge University Press, Cambridge, United Kingdom and New York, NY, USA.

IPCC, 2013: Climate Change 2013. The Physical Science Basis. Contribution of Working Group I to the Fifth Assessment Report of the Intergovernmental Panel on Climate Change. Stocker, T.F., Qin, D., Plattner, G.-K., Tignor, M., Allen, S.K., Boschung, J., Nauels, A., Xia, Y., Bex, V., and Midgley, P.M., eds., (2013). Cambridge University Press, Cambridge, United Kingdom and New York, NY, USA, pp. 1535.

IPCC, 2013: Climate Change 2013. The Physical Science Basis. Contribution of Working Group I to the Fifth Assessment Report of the Intergovernmental Panel on Climate Change. Ciais, P., Sabine, C., Bala, G., Bopp, L., Brovkin, V., Canadell, J., Chhabra, A., DeFries, R., Galloway, J., Heimann, M., Jones, C., Le Quéré, C., Myneni, R.B., Piao, S., and Thornton, P.,

(2013). *Carbon and Other Biogeochemical Cycles*. Cambridge University Press, Cambridge, United Kingdom and New York, NY, USA.

Jackson, R.B., Banner, J.L., Jobbágy, E.G., Pockman, W.T., and Wall, D.H., (2002). Ecosystem carbon loss with woody plant invasion of grasslands. *Nature*, 418, 623-626.

Jacobson, M., Charlson, R.J., Rodhe, H., and Orians, G.H., (2000). *Earth System Science: from biogeochemical cycles to global changes*. Academic Press, San Diego, California.

Jeltsch, F., Weber, G.E., and Grimm, V., (2000). Ecological buffering mechanisms in savannas: A unifying theory of long-term tree-grass coexistence. *Plant Ecology*, 150(1-2), 161–171.

Jobbágy, E.G., and Jackson, R.B., (2000). The vertical distribution of soil organic carbon and its relation to climate and vegetation. *Ecological Applications*, 10(2), 423–436.

Jonckheere, I., Fleck, S., Nackaerts, K., Muys, B., Coppin, P., Weiss, M., and Baret, F., (2004). Methods for leaf area index determination. Part I: Theories, techniques and instruments. *Agricultural and Forest Meteorology*, 121(1-2), 19–35.

Kassahuna, A., Snyman, H.A., and Smit, G.N., (2008). Impact of rangeland degradation on the pastoral production systems, livelihoods and perceptions of the Somali pastoralists in Eastern Ethiopia. *Journal of Arid Environments* 72(7), 1265–1281.

Lix, L.M., Keselman, J.C., and Keselman, H.J., (1996). Consequences of assumption violations revisited: A quantitative review of alternatives to the one-way analysis of variance *F* test. *Review of Educational Research*, Vol. 66(4), 579–619.

- Lohmann, D., Tietjen, B., Blaum, N., Joubert, D.F., and Jeltsch, F., (2012). Shifting thresholds and changing degradation patterns: climate change effects on the simulated long-term response of a semi-arid savanna to grazing. *Journal of Applied Ecology*, 49, 814–823.
- Lu, D., (2006). The potential and challenge of remote-sensing based biomass estimation. *International Journal of Remote Sensing*, 27(7), 1297–1328.
- Marchant, R., Mumbi, C., Behera, S., and Yamagata, T., (2007). The Indian Ocean dipole – the unsung driver of climatic variability in East Africa. *African Journal of Ecology*, 45(1), 4–16.
- McCarthy, N., Kamara, A., and Kirk, M., (2001). The effect of environmental variability on livestock and land-use management: The Borana Plateau, southern Ethiopia. *Environment and Production Technologie Division Discussion Paper 75*. IFPRI, Washington, DC, USA.
- Michelsen, A., and Rosendahl, S., (1990). The effect of VA mycorrhizal fungi, phosphorus and drought stress on the growth of *Acacia nilotica* and *Leucaena leucocephala* seedlings. *Plant and Soil*, 124(1), 7–13.
- Moleele, N.M., Ringrose, S., Matheson, W., and Vanderpost, C., (2002). More woody plants? The status of bush encroachment in Botswana's grazing areas. *Journal of Environmental Management*, 64(1), 3–11.
- Northup, B.K., Zitzer, S.F., Archer, S., McMurtry, C.R., and Boutton, T.W., (2005). Above-ground biomass and carbon and nitrogen content of woody species in a subtropical thornscrub parkland. *Journal of Arid Environments*, 62, 23–43.
- Oldeland, J., Dorigo, W., Wesuls, D., and Jürgens, N., (2010). Mapping bush encroaching species by seasonal differences in Hyperspectral Imagery. *Remote Sensing*, 2, 1416–1438.

- Otieno, D.O., Kinyamario, J.I., and Omenda, T.O., (2001). Growth features of *Acacia tortilis* and *Acacia xanthophloea* seedlings and their response to cyclic soil drought stress. *African Journal of Ecology*, 39(2), 126–132.
- Piepho, H.-P., (2008). Statistik für Studierende im B.Sc. Agrarbiologie (AB) and im B.Sc. Nachwachsende Rohstoffe (NaWaRo) an der Universität Hohenheim, 1. Semester (AB), 3. Semester (NaWaRo). Institut für Pflanzenbau and Grünland (340), FG Bioinformatik, Universität Hohenheim.
- Poupon, H., (1977). Production de matière sèche d` *Acacia Senegal* (L.) Willd. dans une savane sahélienne au Sénégal. *International Journal of Tropical Geology, Geography and Ecology*, 3, 209–228.
- Prather, M., Holmes, C., and Hsu, J., (2012). Reactive greenhouse gas scenarios: Systematic exploration of uncertainties and the role of atmospheric chemistry. *Geophysical Research Letter*, 39(9).
- Privette, J.L., Tian, Y., Roberts, G., Scholes, R.J., Wang, Y., Caylor, K.K., Frost, P., and Mukelabai, M., (2004). Vegetation structure characteristics and relationships of Kalahari woodlands and savannas. *Global Change Biology*, 10(3), 281–291.
- Prodanov, D., (2003). Grayscale Morphology. URL: <http://rsb.info.nih.gov/ij/plugins/gray-morphology.html> (State: 04.08.2014).
- Randerson, J.T., Chapin, F.S., Harden, J.W., Neff, J.C., and Harmon, M.E., (2002). Net ecosystem production: A comprehensive measure of net carbon accumulation by ecosystems. *Ecological Applications*, 12(4), 937–947.

Raupach, M.R., Marland, G., Ciais, P., Le Quéré, C., Canadell, J.G., Klepper, G., and Field, C.B., (2007). Global and regional drivers of accelerating CO₂ emissions. *PNAS*, *104*(24), 10288–10293.

Reid, R.S., Kruska, R.L., Muthui, N., Taye, A., Wotton, S., Wilson, C.J., and Mulatu, W., (2000). Land-use and land-cover dynamics in response to changes in climatic, biological and socio-political forces: the case of southwestern Ethiopia. *Landscape Ecology*, *15*, 339–355.

Ryu, Y., Nilson, T., Kobayashi, H., Sonnentag, O., Law, B.E., and Baldocchi, D.D., (2010). On the correct estimation of effective leaf area index: Does it reveal information on clumping effects? *Agricultural and Forest Meteorology*, *150*(3), 463–472.

Sampson, D.A., and Allen, H.L., (1995), Direct and indirect estimates of Leaf Area Index (LAI) for lodgepole and loblolly pine stands. Springer-Verlag, *Trees*, *9*, 119–122.

Sankaran, M., Hanan, N.P., Scholes, R.J., Ratnam, J., Augustine, D.J., Cade, B.S., Gignoux, J., Higgins, S.I., Le Roux, X., Ludwig, F., Ardo, J., Banyikwa, F., Bronn, A., Bucini, G., Caylor, K.K., Coughenour, M.B., Diouf, A., Ekaya, W., Feral, C.J., February, E.C., Frost, P. G.H., Hiernaux, P., Hrabar, H., Metzger, K.L., Prins, H.H.T., Ringrose, S., Sea, W., Tews, J., Worden, J., and Zambatis, N., (2005). Determinants of woody cover in African savannas. *Nature*, *438*, 846–849.

Schaphoff, S., Lucht, W., Gerten, D., Sitch, S., Cramer, W., and Prentice, C., (2006). Terrestrial biosphere carbon storage under alternative climate projections. *Climatic Change*, *74*(1-3), 97–122.

Scholes, R.J., Frost, P.G., and Tian, Y., (2004). Canopy structure in savannas along a moisture gradient on Kalahari sands. *Global Change Biology*, *10*(3), 292–302.

Scurlock, J.M.O., and Hall, D.O., (1998). The global carbon sink: a grassland perspective. *Global Change Biology*, 4, 229–233.

Steffen, W., Sanderson, A., Tyson, P., Jäger, J., Matson, P., Moore III, B., Oldfield, F., Richardson, K., Schnellhuber, H.J., Turner II, B., and Wasson, R., (2004). *Global Change and the Earth System. A Planet Under Pressure*. Springer, Berlin.

Subramanian, P., and Sampathrajan, A., (1999). Physical and chemical characterisation of selected weed species for energy production. *Bioresource Technology*, 70(1), 51–54.

Sundquist, E.T., (1990). Influence of deep-sea benthic processes on atmospheric CO₂. *Philosophical Transactions of Royal Society A*, 331(1616), 155-165.

Valentini, R., Arneth, A., Bombelli, A., Castaldi, S., Cazzolla Gatti, R., Chevallier, F., Ciais, P., Grieco, E., Hartmann, J., Henry, M., Houghton, R.A., Jung, M., Kutsch, W.L., Malhi, Y., Mayorga, E., Merbold, L., Murray-Tortarolo, G., Papale, D., Peylin, P., Poulter, B., Raymond, P.A., Santini, M., Sitch S., Vaglio Laurin, G., van der Werf, G.R., Williams, C.A. and Scholes, R.J., (2013). The full greenhouse gases budget of Africa: synthesis, uncertainties and vulnerabilities. *Biogeosciences Discussions*, 10, 8343–8413.

Vitousek, P.M., Mooney, H.A., Lubchenco, J., and Melillo, J.M., (1997). Human domination of Earth's ecosystems. *Science*, 277.

Wang, Y.S., Miller, D.R., Welles, J.M., and Heisler, G.M. (1992). Spatial variability of canopy foliage in an oak forest estimated with fisheye sensors. *Forest Science*, 38(4), 854–865.

Welles, J.M., and Norman, J.M., (1991). Instrument for indirect measurement of canopy architecture. *Agronomy Journal*, 83(5), 818–825.

Wolfinger, R.D., (1996). Heterogeneous variance: covariance structures for repeated measures. *Journal of Agricultural, Biological and Environmental Statistics*, 1(2), 205–230.